united nations educational, scientific and cultural organization

international atomic energy agency

the
abdus salam
international centre for theoretical physics

SMR 1331/17

AUTUMN COLLEGE ON PLASMA PHYSICS

8 October - 2 November 2001

DYNAMIC CURRENT SHEETS - II

Lev Zelenyi

Russian Acedemy of Sciences, Space Research Institute
Moscow, Russia

These are preliminary lecture notes, intended only for distribution to participants.

INTERNATIONAL ATOMIC ENERGY AGENCY
UNITED NATIONS EDUCATIONAL, SCIENTIFIC AND CULTURAL ORGANIZATION
INTERNATIONAL CENTRE FOR THEORETICAL PHYSICS
I.C.T.P., P.O. BOX 586, 34100 TRIESTE, ITALY, CABLE: CENTRATOM TRIESTE

Lecture 1.

CURRENT SHEETS IN SPACE PLASMA

Non adiabatic particle dynamics and
numerical simulations

Lecture 2.

EQUILIBRIUM CONFIGURATIONS OF FORCED SHEETS

Role of trapped and transient populations.

Lecture 3.

FRACTAL STRUCTURES IN CURRENT SHEETS

Multiscale turbulence and current branching

Acknowledgements:

UCLA
V.Peroomian
M.Ashour-Abdalla

Maryland University
D.Schriver
M.Sitnov
S.Sharma

Calabria University
G.Zimbardo
P.Veltri
A.Greko

MPAE, Lindau
J.Büchner

Space Research Institute
A.Galeev
A.Milovanov
H.Malova
E.Grigorenko

Georgian Observatory
A.Taktakishvili

INTERNATIONAL ATOMIC ENERGY AGENCY
UNITED NATIONS EDUCATIONAL, SCIENTIFIC AND CULTURAL ORGANIZATION
INTERNATIONAL CENTRE FOR THEORETICAL PHYSICS
I.C.T.P., P.O. BOX 586, 34100 TRIESTE, ITALY, CABLE: CENTRATOM TRIESTE

Lecture 2.

EQUILIBRIUM CONFIGURATION OF FORCED (ANISOTROPIC) CURRENT SHEETS

1. **Introduction.**
    1. Isotropic and Anisotropic CS.
    2. Experimental observations of thin CS in magnetosphere.

2. **Kinetic properties of CS**
    1. Structure of the phase space
    2. Nonadiabatic trajectories and structure of currents.
    3. DIA – and PARAMAGNETIC currents in plasma.
    4. Phase mixing and trapped population.

3. **Equilibrium solutions in quasiadiabatic approximation**
    1. Limits of quasiadiabaticity
    2. Plasma sources (mantle)
    3. Basic equation and Liouville theorem
    4. Grad-Shafranov equations for plasma equilibrium.
    5. Limits of weak and strong anisotropies.
    6. Nonadiabatic effects for superstrong anisotropy.
    7. Scaling of CS thickness.

4. **Influence of electric fields and Speiser acceleration.**
    1. Nonadiabatic acceleration.
    2. Thinning of CS

5. **Trapped population and windows for the existence of equilibrium solutions**

6. **Conclusions:** Possible scenarios of Disruption

Formation of current sheet structure due to interaction of the impinging plasma beams

Models of sheet

- *Eastwood*, [1972,1974]
  First studies of structure;

  Alexeev and Kropotkin, [1971]
  Step-like field model;

- *Francfort and Pellat*, [1976]
  Analytically: $L=\rho(v_T/v_D)^{4/3}$;

- *Pritchett and Coroniti*, [1992]
  Numerically: $L=\rho(v_T/v_D)^{4/3}$,
  $L\approx\rho(B_n/B_0)^{4/3}$ ($\theta<b_n$).

- *Burkhart et al.*, [1992]
  Strong anisotropy $L\sim(v_T/v_D)^{4/3}$
  catastrophy at $\kappa\to 1$;

- *Holland and Chen*, [1993],
  Harold, Chen, [1996]
  Numerically: weak/strong anisotropy, role of $\vec{M}$, J_D;

  Ashour-Abdalla et al., [1994]
  Estimate L~ρ for weak anisotropy;

  Kropotkin et al., [1997],
  Analitically: $L\sim\varepsilon^{4/3}$.

Related works

Speiser, [1965]
Nonadiabatic orbits;

Sonnerup, [1971]
Calculation of I_z;

Rich et al., [1972]
Stress balance;

Cowley, [1978]
Effect of pressure anisotropy on the equilibrium structure;

Lyons and Speiser, [1985]
Conductivity;

Chen and Palmadesso, [1986]
Buchner and Zelenyi, [1986];
Role of chaos;

Zelenyi and Savenkov, [1993]
Estimate of ΔI_z for $I_z<<\kappa$;

Kaufmann et al., [1993-1998]
Taking into account trapped particles;

Delcourt et al., [1993-1998]
Centrifugally-driven effects;

Hesse, Kusnezova et al., [1997-1999]
The role of electron effects.

EXPERIMENT:

Existence of thin current sheets have been manifested in numerous experimental data:

1. The thin current sheet 0.2 R_E thick is embedded inside a plasma sheet with a thickness about several R_E:

- Sergeev, V.A., V. Angelopoulos, C. Carlson, and P. Sutcliffe, Current sheet measurements within a flapping plasma sheet, J. Geophys. Res., **103**, 9177, 1998.
- Sanny, J., R.L. McPherron, C.T. Russell, D.N. Baker, T.I. Pulkkinen, and A. Nishida, Growth phase thinning of the near-Earth current sheet during the CDAW-6 substorm, J. Geophys. Res., **99**, 5805, 1994.

2. Current sheets with a thickness about ion gyroradius (~400 km) are observed in the near Earth tail during the growth and expansion substorm phases.

- Mitchell, D. et al. Geophys. Res. Lett., **17**, 583, 1990.
- Sergeev, V.A., D.G. Mitchell, C.T. Russell, and D.J. Williams, Structure of the tail plasma/current sheet at 11 Re and its changes in the course of a substorm, J. Geophys. Res., **98**, 17345, 1993
- Pulkkinen, T. I., et al., In: Substorms 1, ESA-SP 335, Noordwijk, TheNetherlands, p. 131, 1992.

3. Thin current sheets are also observed in the distant tail (X>200 Re).

- Pulkkinenn, T.I., et al. Geophys. Res.Lett., **20**, 2427,1993.
- Gosling, J.Geophys.Res., **90**, 6354, 1985.

4. It was found that the thin current sheet is carried by cross tail quasi- adiabatic ions [Pulkkinen et al.,1992; Lui A., JGR,98, 423, 1993].

5. In several experiments TCS are found to display the overshoot structure

Essential experimental properties of CS:
small thickness,
anisotropy, embedding structure,
ions as carrier, presumably overshoot structure.

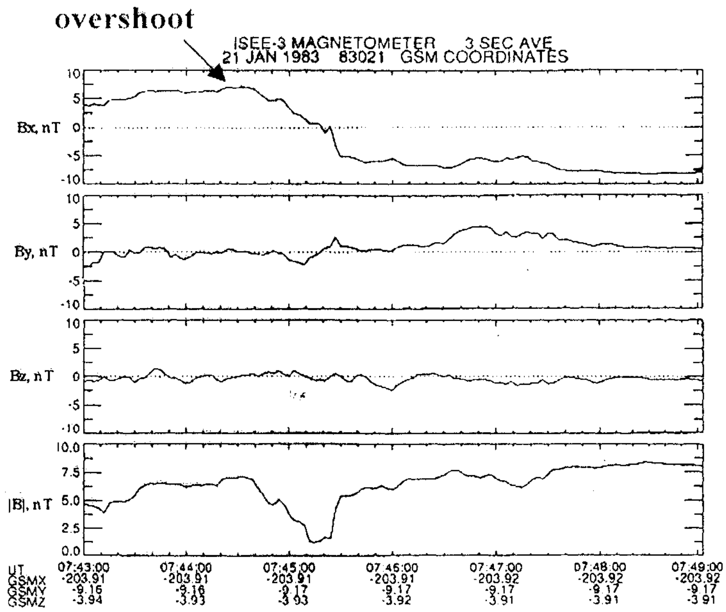

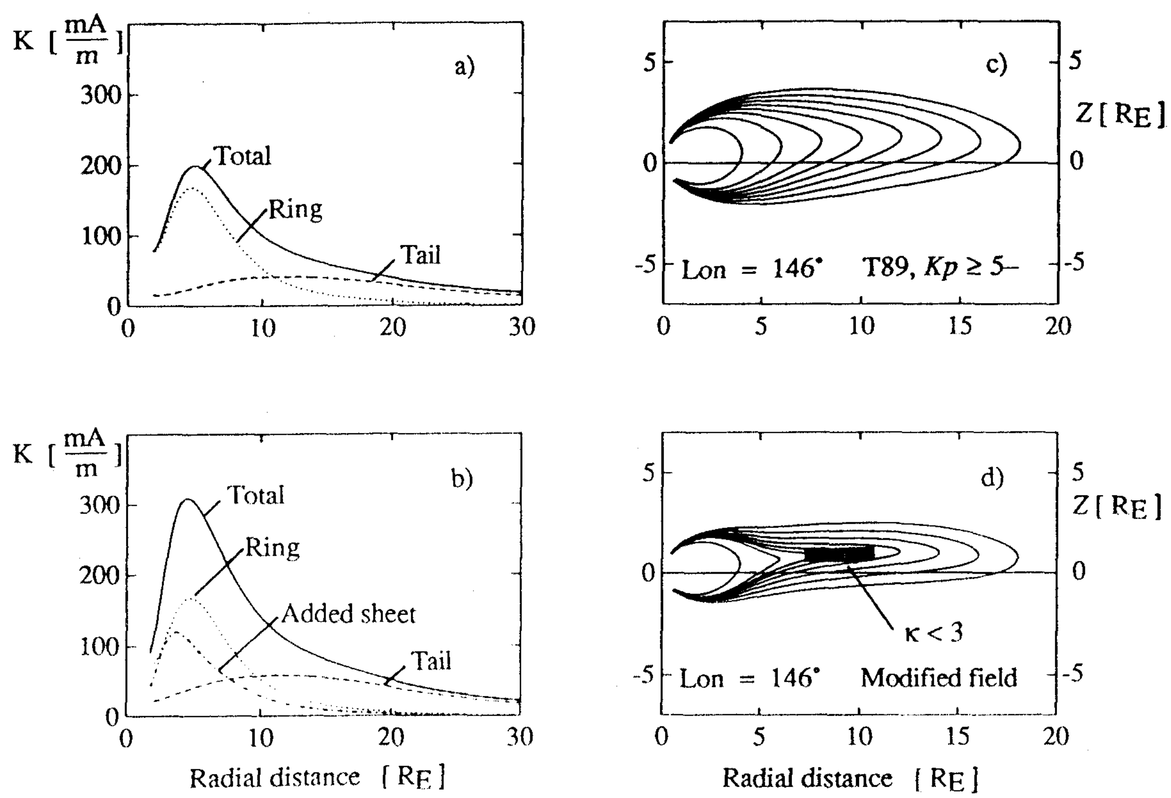

Fig. 9. Left: Current intensities integrated over the current sheet thickness (in mA/m) in the ISEE 1 meridian a) in the basic T89 model, and b) in the modified model of the Pulkkinen et al. (1991). Total current (solid line), tail current (dotted line), and ring current (dashed line) are shown for both cases. The additional current sheet is shown by dash-dotted line. Right: Field line projections to the ISEE 1 meridian computed using c) basic T89 model and d) the modified model. The region of chaotic electron motion for 1 keV electrons (see text) is shown hatched.

magnetic field by gradually increasing the cross-tail current, thinning the current sheet, and adding another localized tail current system with increasing intensity in the basic Tsyganenko model. This gives a global growth phase field model which compares favorably with measurements from several spacecraft in the magnetotail. The modified, time-dependent Tsyganenko model allows a systematic mapping of auroral features recorded by the auroral imagers into the near-tail region. These results, and a mapping study utilizing auroral images from Viking and the Tsyganenko 1987 model (Elphinstone et al., 1990), suggest that the auroral brightenings correspond to regions of thinned and intensified current sheet remarkably close to the Earth.

Specifically, Pulkkinen et al. (1991) include growth phase effects for the event under study by varying the Tsyganenko model parameters and by modification of the functional form of the field components. The current sheet is thinned locally by modification of the X and Y dependent function determining the current sheet thickness in the model (see Pulkkinen 1991) with the minimum thickness, location of the minimum thickness, and size of the thinned region as free parameters. The cross-tail current is intensified by enhancement of the model tail current by a constant factor. However, because the tail current peaks beyond 10 R_E, its enhancement cannot represent stretching of the field in the near-Earth region between 6 and 10 R_E. In order to further enhance stretching close to the Earth, a new thin current sheet is added to the model. The form of the current distribution is similar to the model ring current term, but the peak intensity, location of current maximum, and the current sheet thickness are set according to the observed degree of field stretching.

A time-dependent model for the growth phase was constructed by linearly varying the parameters describing the enhancement of the currents during growth phase until substorm onset. The field at the beginning of the growth phase is represented by the unmodified Tsyganenko model using the highest level of

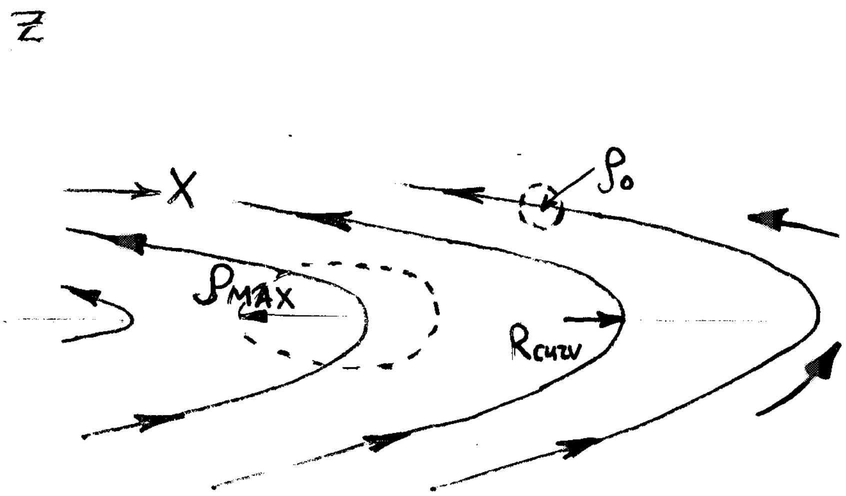

Parameter of Adiabaticity

$$\varkappa = \sqrt{\frac{R_{curv}}{\rho_{MAX}}}$$

(Büchner, Zelenyi: 1986,89)

Quasiadiabatic approximation: $\varkappa \approx \frac{B_n}{B_o}\sqrt{\frac{L}{\rho_{oi}}} < 1$

(Ti ≈ 5keV, L ≈ 3000 km, Bn = 1nT, Bo = 20nT, $\varkappa_i \sim 0.1$)

$\varkappa$ - parameter of smallness

(opposite limit to the Guiding Center Theory: $\varkappa \gg 1$)

Motion could be roughly separated on slow (**x**) and fast (**z**) parts

Action for fast variable $I_z = \frac{1}{2\pi}\oint \dot{z}\, dz$

- **natural invariant** of motion (Speiser 1965, Sonnerup 1970, BZ 1989)

I_z - is conserved only approximately $\left(\frac{\Delta I}{I} \sim \varkappa\right)$

QUASIADIBATIC APPROXIMATION : $I_z = \text{const}$

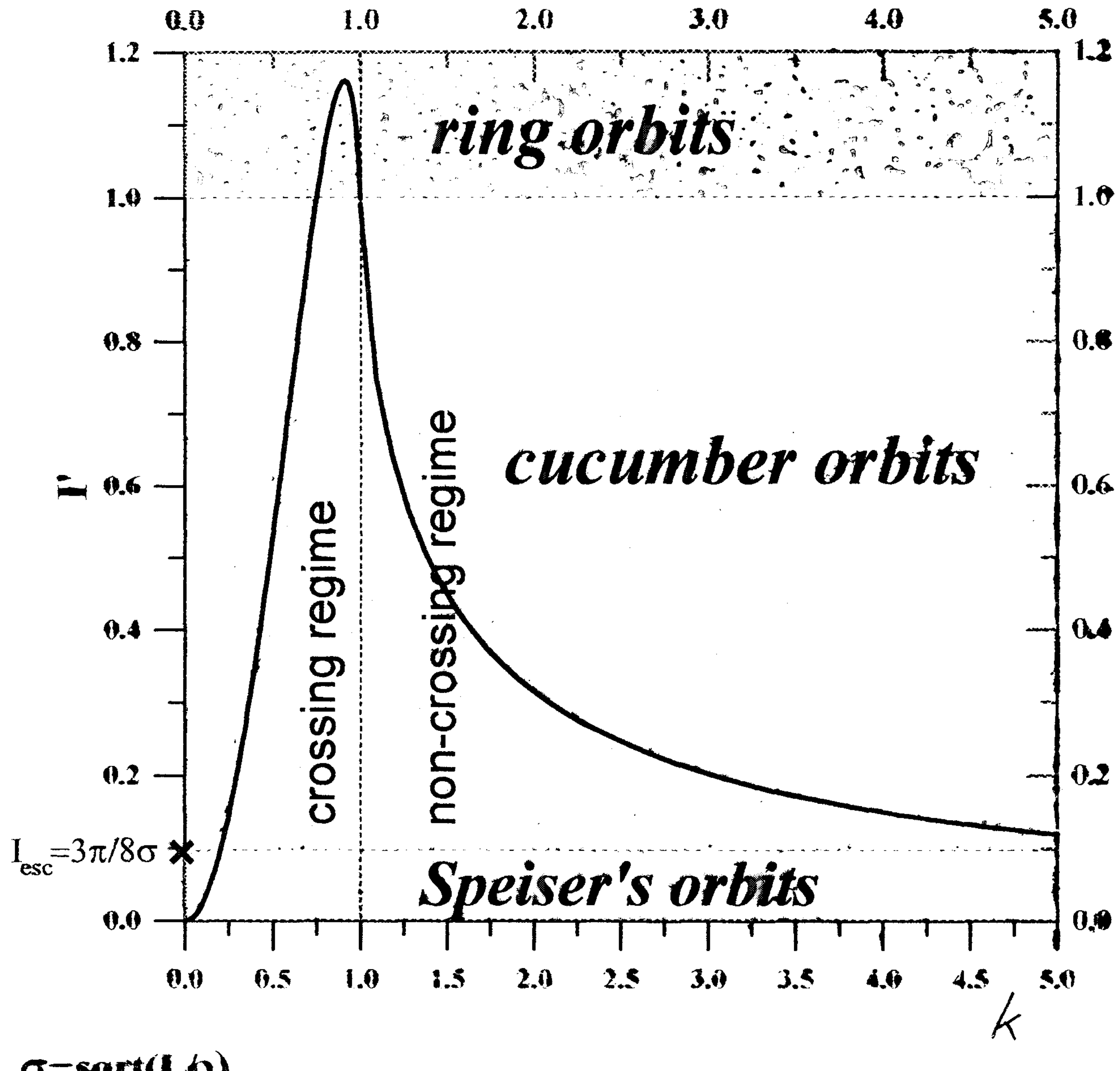

ring orbits
cucumber orbits
crossing regime
non-crossing regime
Speiser's orbits
$I_{esc}=3\pi/8\sigma$
I'
k

σ=sqrt(L/ρ)

The principal types of ion trajectories in TCS (X-Z plane) and corresponding current densities $j_y(Z)$

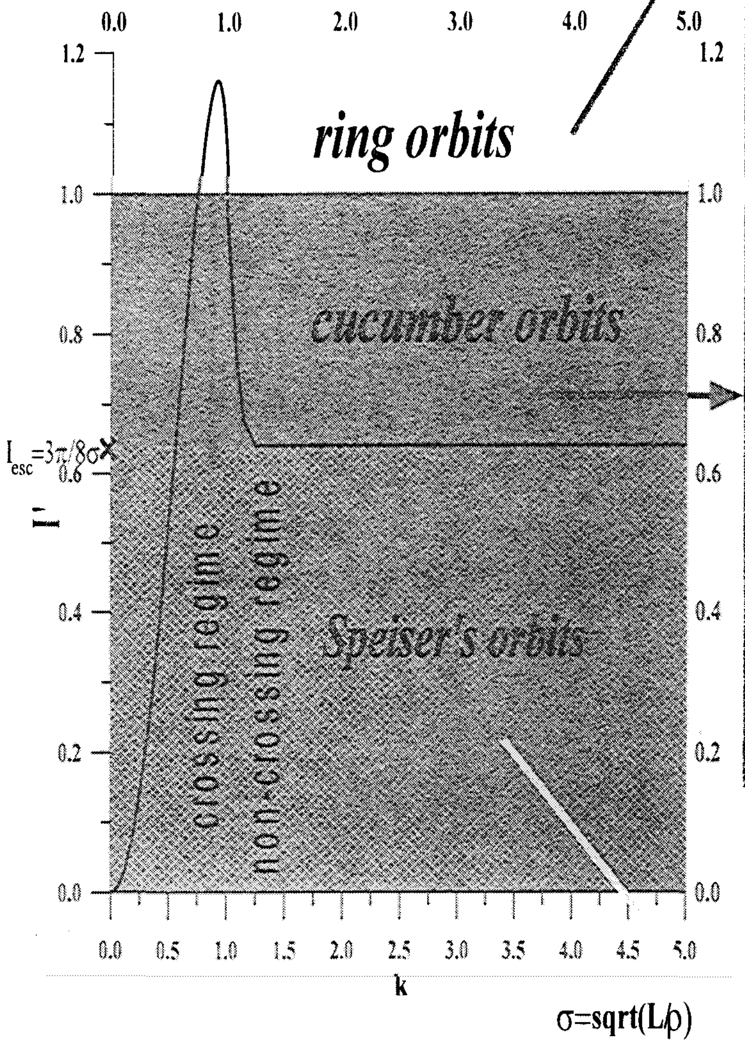

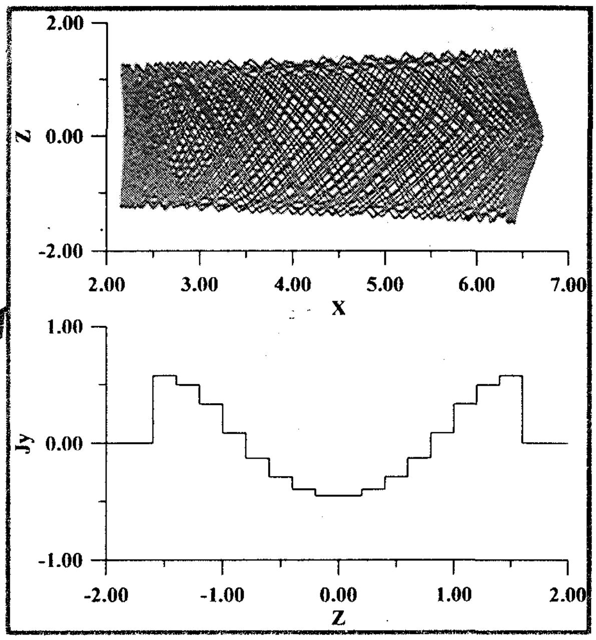

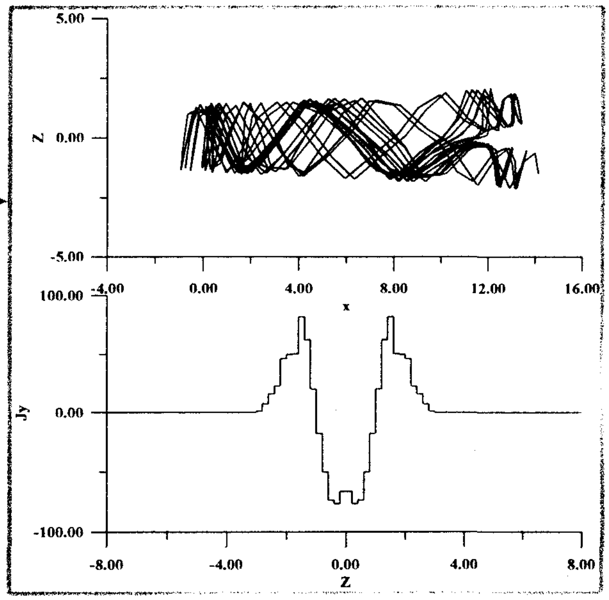

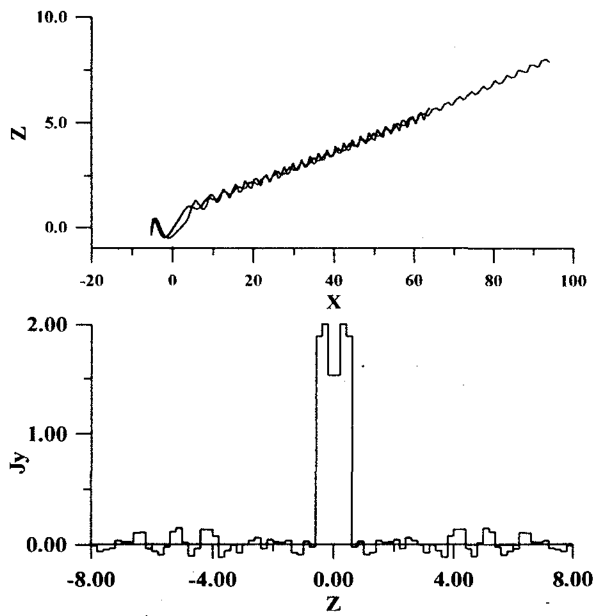

THE PARTIAL CURRENTS AND MAGNETIC FIELDS OF THE TRAPPED POPULATION

Partial current densities of transient and trapped populations

ε=10, κ=1

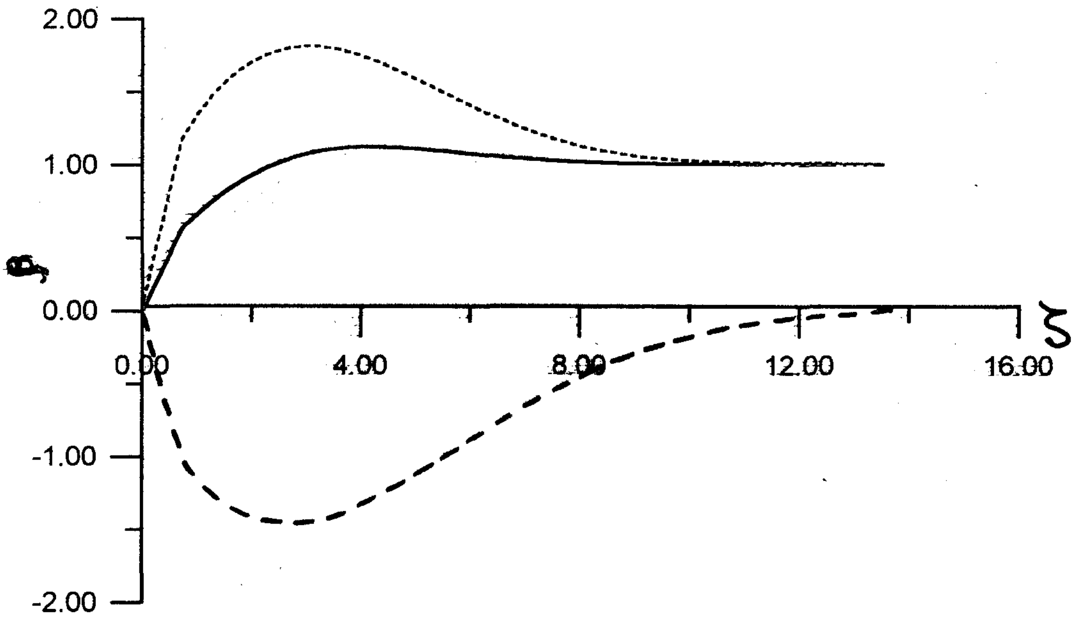

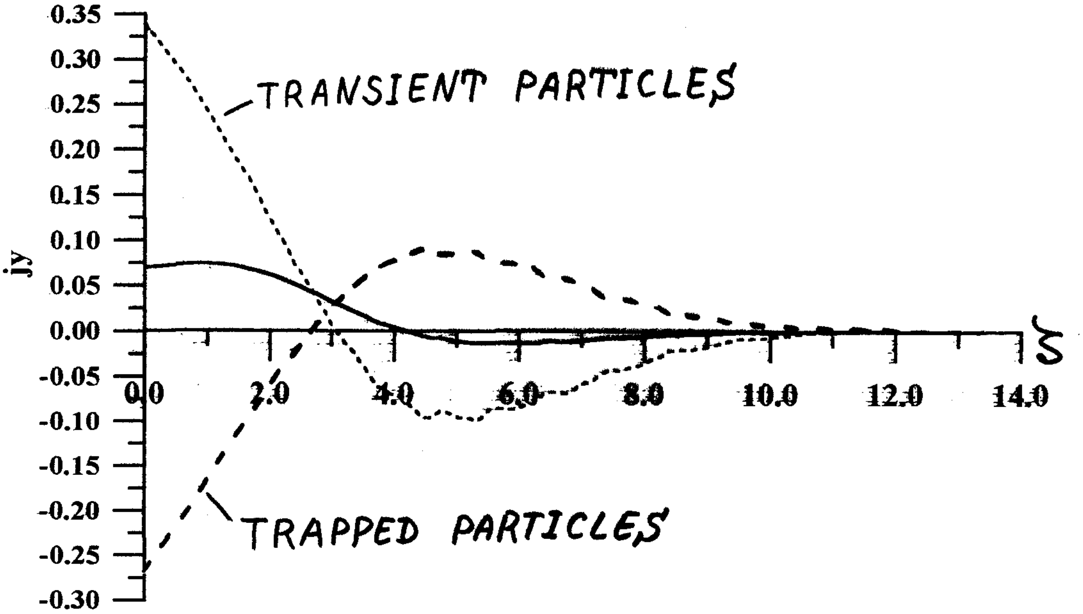

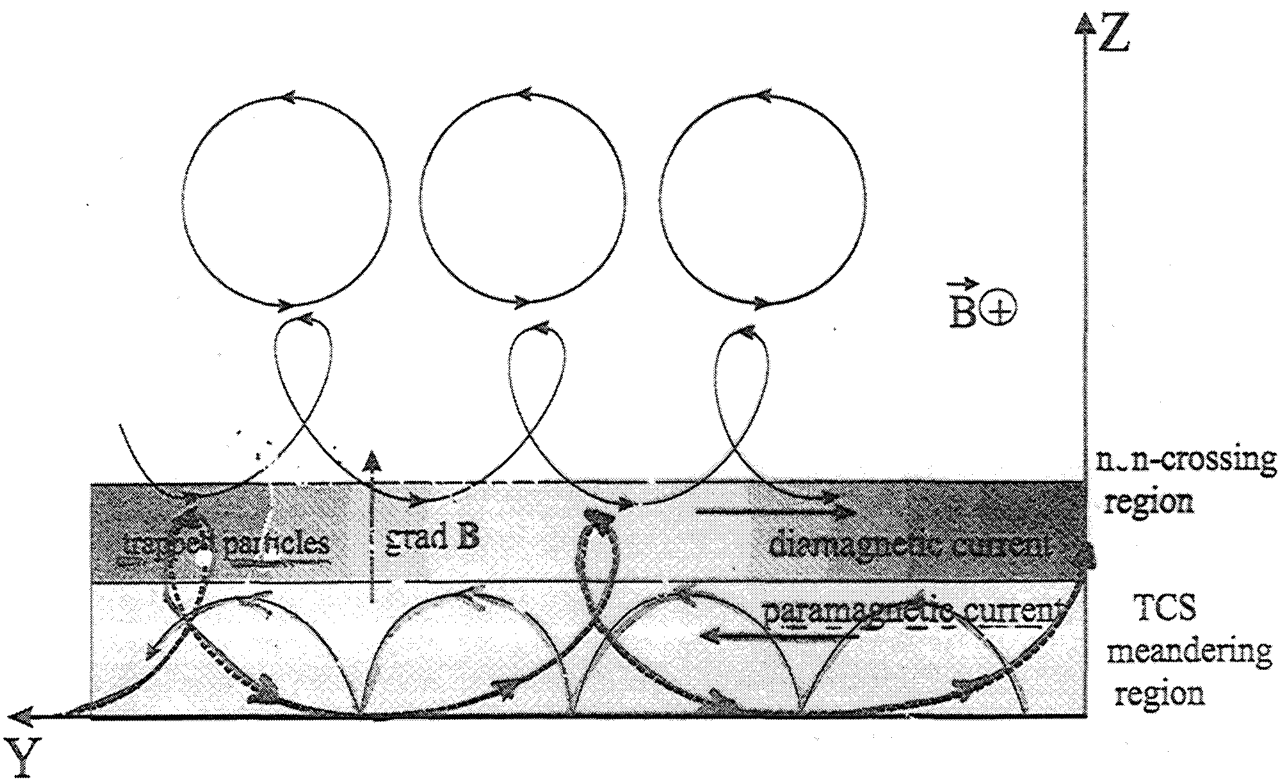
Z
$\vec{B}\oplus$
n.n-crossing
region
trapped particles
grad B
diamagnetic current
paramagnetic current
TCS
meandering
region
Y

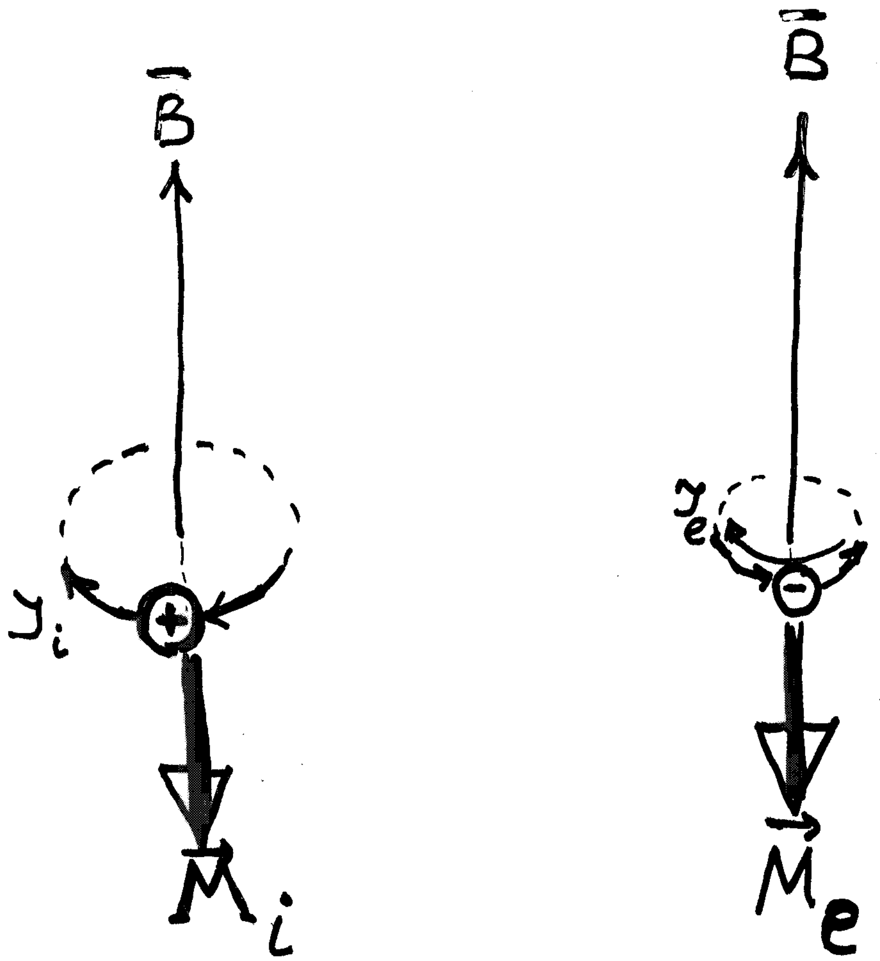

MAGNETIZED PLASMA

IS <u>DIAMAGNETIC</u>

Paramagnetic current - as an EDGE effect

$$\bar{M}_{DIA} = -\frac{P_\perp \bar{B}}{|\bar{B}|^2}$$

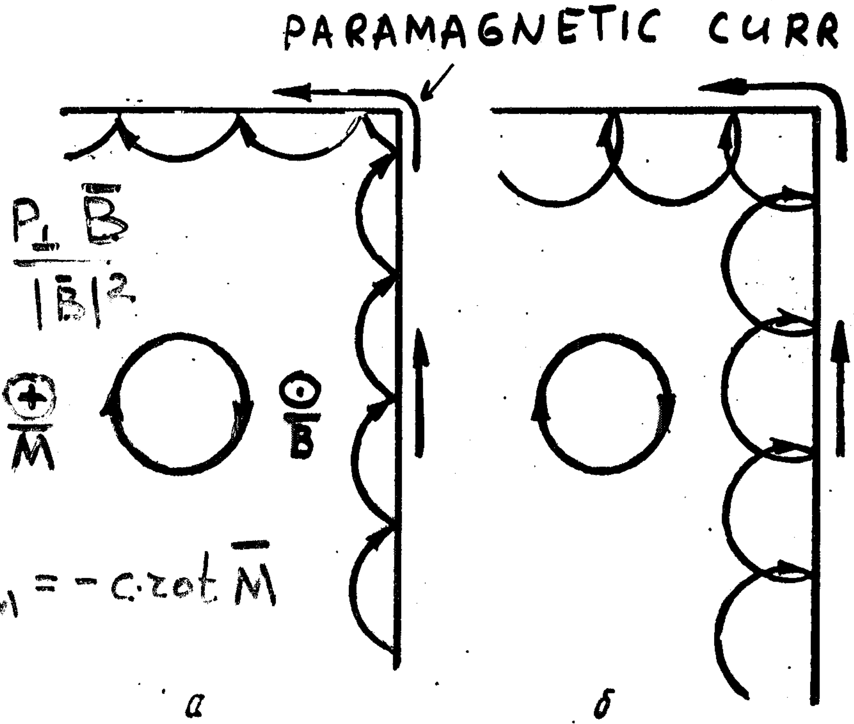

$$\bar{M}_{PAR} = \alpha \frac{P_\perp \bar{B}}{|\bar{B}|^2}$$

$$0 < \alpha \leq 1$$

$$\bar{J}_M = -c \cdot \mathrm{rot}\, \bar{M}$$

Рис. 9. Краевой парамагнитный ток при упругом отражении частиц:
а — отражение под острым углом; б — отражение под тупым углом.

$$\bar{B} = \bar{H} + 4\pi \bar{M}_{DIA} + 4\pi \bar{M}_{PAR}$$

FRANK-KAMENETSKY

BASICS

Forced current sheet is formed by interaction of impinging ion beams. Principal difference from HARRIS equilibrium.

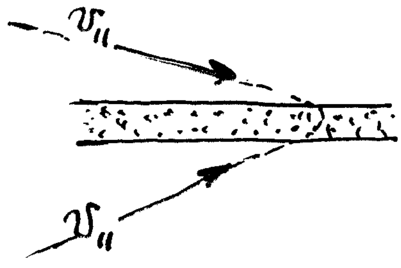

Assumptions:

- **1D** $\left(\frac{\partial}{\partial x}=\frac{\partial}{\partial y}=0\right)$
- **Ion dominated CS**
- **B_n=const$\neq$0 (quasineutral sheet)**
- **Quasiadiabaticity** $I_z=\frac{1}{2\pi}\oint \dot{z}dz \cong const$
- **Contibutions from the transient and trapped orbits**
- **Phase mixing of trapped population**

⇩

GRAD-SHAFRANOV description for self-consistent equilibria

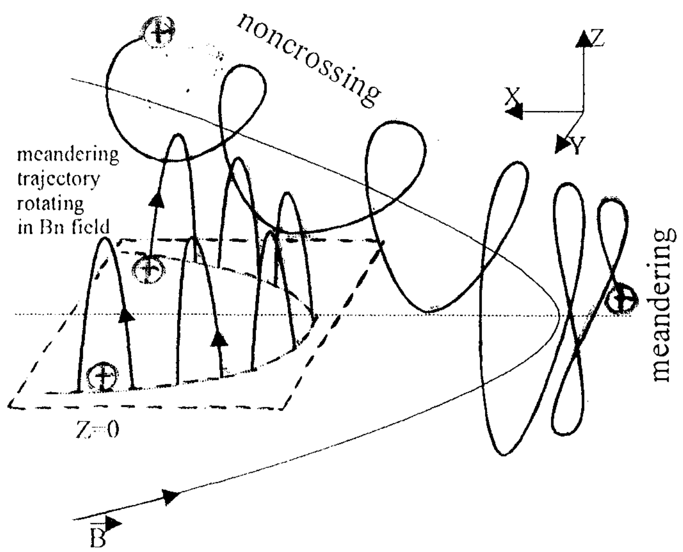

THE THEORY OF THIN CURRENT SHEETS (TCSs)

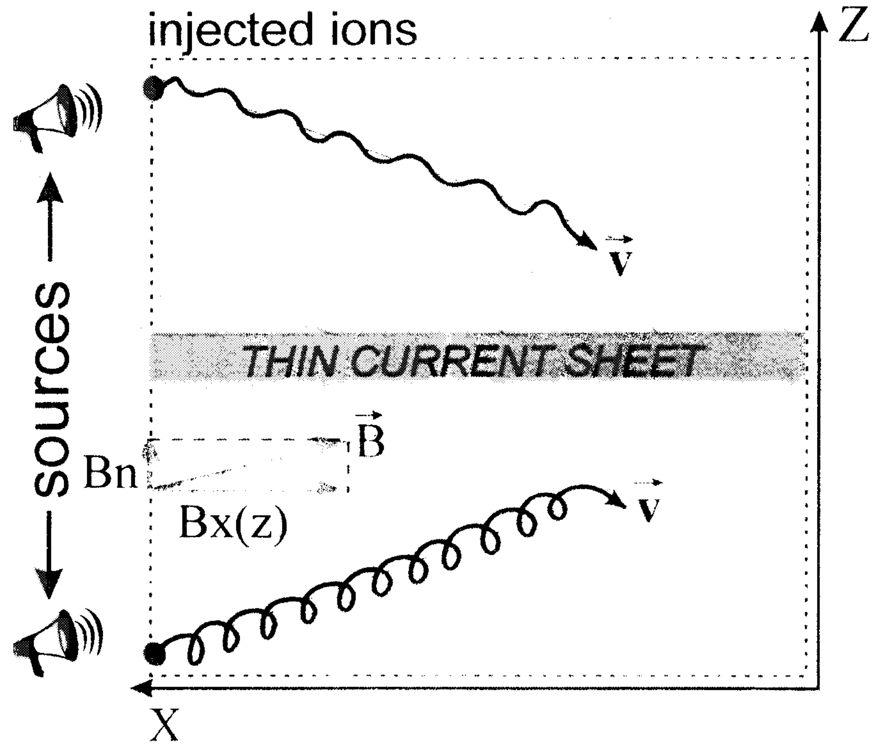

$$\vec{B} = \{B_x(z), 0, B_n\}$$

$B_x(z) = -B_x(-z)$;

$\varepsilon = v_T/v_D$ is the measure of ion streaming;

v_T is the thermal velocity;

v_D is the flow drift velocity

Equations of particle motion:

$$m\ddot{\vec{r}} = \frac{e}{c}\left[\vec{v} \times \vec{B}\right] \qquad (1)$$

$$\begin{cases} \dot{v}_x = \dfrac{e}{mc} v_y B_n \\ \dot{v}_y = \dfrac{e}{mc}\left(v_z B(z) - v_x B_n\right) \\ \dot{v}_z = -\dfrac{e}{mc} v_y B(z) \end{cases} \qquad (2)$$

EXACT INTEGRALS OF MOTION:

1. *Total energy*- $W_0 = \dfrac{mv_0^2}{2}; \quad v_0^2 = v_x^2 + v_y^2 + v_z^2$ (3)

2. *Generalized momentum* ($\partial / \partial y = 0$)

$$mV_y = mv_y - \frac{e}{c}A_y(x,z), \quad A_y(x,z) = -\int_0^z B(z')dz' + B_n x \quad (4)$$

$$\text{æ} = \sqrt{R_c / \rho_L} << 1 \Rightarrow \langle \omega_z \rangle / \langle \omega_x \rangle >> 1$$

$\Rightarrow$ Motions could be decoupled

Therefore action integral of fast motion I_z is conserved:

$$I_z \equiv \frac{1}{2\pi} \oint mv_z dz \approx const \quad (5)$$

Substituting (3) and (4) in (5) we receive

$$\boxed{\begin{aligned} I_z &= \frac{m}{2\pi}\oint\sqrt{v_0^2 - v_x^2 - \left(V_y - \frac{e}{mc}A_y(x,z)\right)^2}\,dz' = \\ &= \frac{m}{2\pi}\oint\sqrt{v_0^2 - v_x^2 - \left(v_y + \frac{e}{mc}\left(A_y(x,z) - A_y(x,z')\right)\right)^2}\,dz' \end{aligned}} \quad (6)$$

CALCULATION of I_z

Due to homogeneity of TCS along *X* direction we have from (4)

$$A_y(x,z) - A_y(x,z') = \int_z^{z'} B(z')dz' \tag{7}$$

Eq.(7) does not depend explicitly on *X*.
Finally, expression for adiabatic invariant I_z is:

$$\boxed{I_z(z,\vec{v}) = \frac{m}{2\pi}\oint\sqrt{v_0^2 - v_x^2 - \left(v_y - \frac{e}{mc}\int_{z'}^{z} B(z'')dz''\right)^2}\, dz'} \tag{8}$$

Limits of integration

$\oint\sqrt{\ldots} \equiv 2\int_{z_1}^{z_2}\sqrt{\ldots}$; limits of integration in (8) $z_1(z, v_y, v_z)$ and $z_2(z, v_y, v_z)$ are determined accordingly to Eq.(8)

$$v_z = 0 \tag{9}$$

$$v_0^2 - v_x^2 - \left(v_y - \frac{e}{mc}\int_{z'}^{z} B(z'')dz''\right)^2 = 0 \tag{10}$$

$$\Downarrow$$

z_1 and z_2 are the solutions of the equation

$$\boxed{\frac{e}{mc}\int_z^{z_{1,2}} B(z'')dz'' = -v_y \pm \sqrt{v_y^2 + v_z^2}} \tag{11}$$

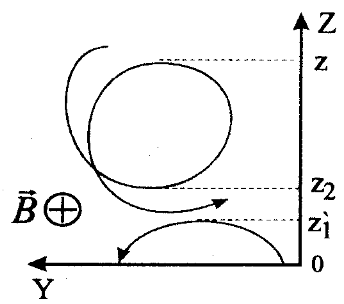

DISTRIBUTION FUNCTION

Distribution function of the injected ions (source) is a shifted Maxwellian

$$\boxed{f(\vec{v}) = \frac{n_0}{\left(\sqrt{\pi} v_T\right)^3} \exp\left\{-\frac{\left(v_{II} - v_D\right)^2}{v_T^2} - \frac{v_\perp^2}{v_T^2}\right\}} \qquad (12)$$

v_{II} and $v_\perp$ are parallel and perpendicular components of $\vec{v}$ along and across $\vec{B}$:

$$v_{II}^2 + v_\perp^2 = v_0^2 \qquad (13)$$

Two examples of the source distribution functions

1. $\varepsilon_1 = v_{T1}/v_{D1} < 1$ (strong anisotropy),
2. $\varepsilon_2 = v_{T2}/v_{D2} > 1$ (weak anisotropy)

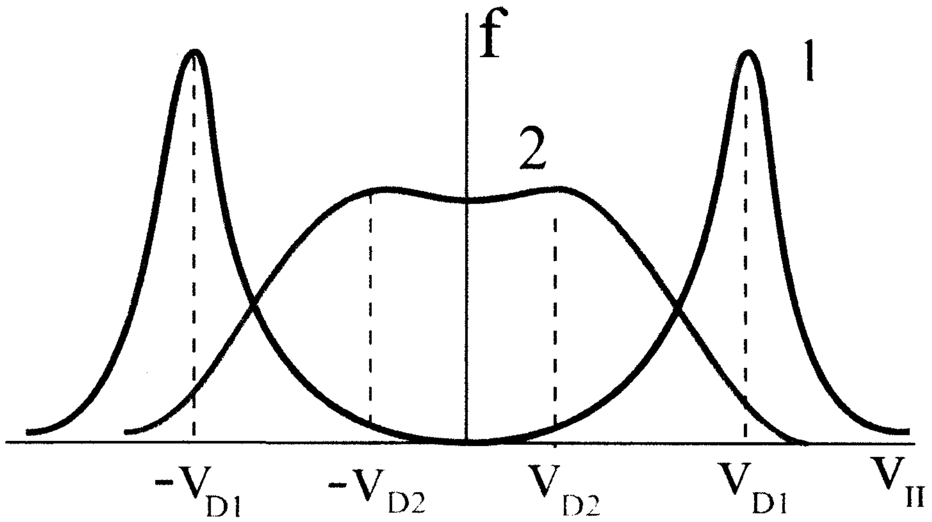

EXPRESSION FOR $f(I_Z, v_0)$

In the region of strong $|\vec{B}|$ the I_z can be easily calculated:

$$I_z = \frac{m}{2\pi}\oint v_z dz$$

$$\approx \frac{m}{2\pi} v_\perp \int_0^{2\pi} r d\phi = \frac{m}{2\pi} v_\perp \frac{v_\perp}{\omega_0} 2\pi \quad = \frac{m v_\perp^2}{\omega_0}$$

Therefore,

$$v_\perp^2 \approx \frac{\omega_0 I_z}{m} \tag{14}$$

$$f(\vec{v}) = \frac{n_0}{\left(\sqrt{\pi} v_T\right)^3} \exp\left\{ - \frac{\left(\sqrt{v_0^2 - \frac{\omega_0 I_z}{m}} - v_D\right)^2}{v_T^2} - \frac{\omega_0 I_z}{m v_T^2} \right\} \tag{15}$$

For $|z| \sim L$ *, where* $|\vec{B}|$ *is large, the motion is magnetized and the adiabatic invariant* I_z *is equivalent to the magnetic moment* $\mu = \frac{m v_\perp^2}{2B}$*. Therefore*

$$I_z = \frac{2mc}{e}\mu \tag{16}$$

However, during crossings of the neutral sheet (z=0) I_z *is approximately conserved, otherwise,* μ *experiences strong jumps.*

LIOUVILLE'S THEOREM

Distribution function in phase space

$$F(p_1, p_2, \dots, p_S, q_1, q_2, \dots, q_S, t)$$

$$\frac{dF}{dt} \equiv \frac{\partial f}{\partial t} + \sum_{j=1,S} \left(\dot{q}_j \frac{\partial f}{\partial q_j} + \dot{p}_j \frac{\partial f}{\partial p_j} \right) = 0$$

$$f(\vec{r}, \vec{v}, t)$$

$$\frac{df}{dt} = \frac{\partial f}{\partial t} + \vec{v}\vec{\nabla} f + \frac{e}{m}\left\{ \vec{E} + \frac{1}{c}\left[\vec{v} \times \vec{H}\right] \right\} \frac{\partial f}{\partial \vec{v}} = St\{f\} = 0$$

$$\boxed{f(I_1, \dots, I_s) = cons}$$

APPLICATION OF THE LIOUVILLE THEOREM TO 1D TCS MODEL

Vlasov-Maxwell system for one-dimensional TCS

$$\frac{dB}{dz} = \frac{4\pi e}{c} \int_V f(z,\vec{v}) v_y d^3 v \qquad (19)$$

We substitute in (19) the distribution function (16) taking into account two independent integrals of motion $\{v_0, I_z\}$:

$$f(z,\vec{v}) = f\big(v_0, I_z(z,\vec{v})\big) = const \qquad (20)$$

Introducing the new variables

$$= z\frac{\omega_0}{\varepsilon^{4/3} v_D}, b = B/B_0, \vec{w} = \vec{v}\frac{1}{\varepsilon^{2/3} v_D}, \varepsilon = \frac{v_T}{v_D} \qquad (21)$$

we obtain from (19):

$$\frac{db}{d\zeta} = \frac{\varepsilon}{\pi^{3/2}} \left(\frac{v_D}{v_A}\right)^2 \int_W w_y \exp\left\{ -\left(\sqrt{\frac{w_0^2}{\varepsilon^{2/3}} - j} - \frac{1}{\varepsilon} \right)^2 - j \right\} d^3 w \qquad (22)$$

where j is the dimensionless adiabatic invariant I_z

$$j = \frac{1}{2\pi} \oint \sqrt{w_0^2 - w_x^2 - \left(w_y - \varepsilon^{2/3} \int_{\zeta'}^{\zeta} b(\zeta'') d\zeta'' \right)^2} \, d\zeta' \qquad (23)$$

GRAD-SHAFRANOV EQUATION FOR COLLISIONLESS PLASMA EQUILIBRIA

Using in (22) the new variable, i.e. vector potential $\boxed{\eta = \varepsilon^{2/3}\int_0^{\zeta} b(\zeta')d\zeta'}$ we obtain *Grad-Shafranov equation* for plasma equilibrium

$$\boxed{b^2(\eta) = \frac{8\varepsilon^{1/3}}{\pi^{3/2}}\left(\frac{V_D}{V_A}\right)^2 \frac{F_{(+)}(\eta) + F_{(-)}(\eta)}{1 + erf(\varepsilon^{-1})}} \tag{24}$$

where

$$I_{(\pm)} = \frac{2}{\pi}\int_{\eta_{0\pm}}^{\eta_{\pm}} \sqrt{\xi^2 - (\pm w_y + \eta''' - \eta')^2}\,\frac{d\eta'''}{b(\eta''')};$$

$$F_{(\pm)}(\eta) = \pm\int_0^{\eta} d\eta' \int_0^{\infty} dw_x \int_0^{\infty} w_y dw_y \int_{w_y}^{\infty} \frac{\xi d\xi}{\sqrt{\xi^2 - w_y^2}}$$

$$\exp\left(-\varepsilon^{-2/3}\left\{\left[\sqrt{\xi^2 + w_x^2 - I_{\pm}} - \varepsilon^{-2/3}\right]^2 + I_{\pm}\right\}\right)$$

Boundary condition:

$$b(\eta_{boundary}) = 1 \tag{25}$$

Undetermined parameter v_A/v_D could be found from boundary condition (25):

$$\frac{v_A}{v_D} = \frac{2\sqrt{2}}{\pi^{3/4}} \frac{\varepsilon^{1/6}}{\sqrt{1 + erf(\varepsilon^{-1})}} \times \sqrt{\int_0^\infty d\eta' \left(F_{(+)}(\eta', w_x) + F_{(-)}(\eta', w_x)\right)} \tag{26}$$

Simplified form of pressure balance along X axis was found by *Burkhart et al.* (1992):

$$\frac{v_A}{v_D} = \left(1 + \frac{\varepsilon}{\sqrt{\pi}} \frac{\exp\left[-\varepsilon^{-2}\right]}{1 + erf(\varepsilon^{-1})}\right)^{1/2} \tag{27}$$

This is equivalent to *marginal firehose stability condition* by Rich *et al.* (1972)

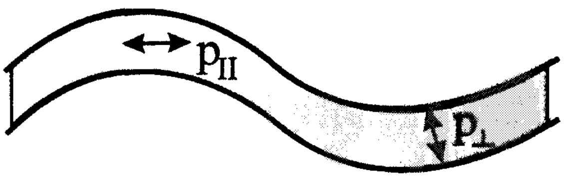

$$p_{II} - p_\perp = \frac{B_0^2}{8\pi} \tag{28}$$

Here p_{II} and $p_\perp$ are the parallel and perpendicular components of the plasma pressure outside the current sheet.

Equation for the pressure balance

Flux of momentum p_x out of the sheet is balanced with the field line tension force $F_x = (B_z/4\pi)dB_x/dz$.

This balance after integrating over the height of TCS

$$\hat{B}_x\hat{B}_z = \int_{\hat{v}_{II}<0} \hat{v}_x\hat{v}_z f_{in} d^3\hat{v} + \int_{\hat{v}_{II}>0} \hat{v}_x\hat{v}_z f_{out} d^3\hat{v}$$

where ^ signifies the normalized variables (see Burkhart *et al.*, 1992) $\hat{v} = v/v_T$, $\hat{B} = B/\sqrt{4\pi n m_i v_T^2}$.

In the absence of scattering

$$f_{in} = f_{out} \sim \exp\{-\hat{v}_\perp^2 - (\hat{v}_{II}^2 - \hat{v}_D^2)^2\}. \qquad (29)$$

Converting to pitch angle, gyrophase coordinates and integrating over phase on can obtain:

$$\hat{B}^2 = \int_{v_{II}<0} \hat{v}_\perp d\hat{v}_\perp d\hat{v}_{II} (\hat{v}_{II}^2 - v_\perp^2/2) f_{in}(\hat{v}_\perp, \hat{v}_{II}) +$$

$$\int_{v_{II}>0} \hat{v}_\perp d\hat{v}_\perp d\hat{v}_{II} (\hat{v}_{II}^2 - v_\perp^2/2) f_{out}(\hat{v}_\perp, \hat{v}_{II}) = p_{II} - p_\perp$$

Taking into account the incoming and outcoming distribution functions (29) we find that

$$\hat{B}^2 = \hat{v}_D^2 + \left[\frac{\hat{v}_D^2}{1 + erf(\hat{v}_D)}\right]\left(\frac{\exp(-\hat{v}_D^2)}{\pi^{1/2}}\right)$$

$$\Downarrow$$

$$\boxed{\frac{v_A}{v_D} = \left(1 + \frac{\varepsilon}{\sqrt{\pi}} \frac{\exp\left[-\varepsilon^{-2}\right]}{1 + erf(\varepsilon^{-1})}\right)^{1/2}}$$

COMPARISON OF THE PRESSURE BALANCE CONDITIONS *(analytical Eq.(26) and numerical Eq. (27))*.

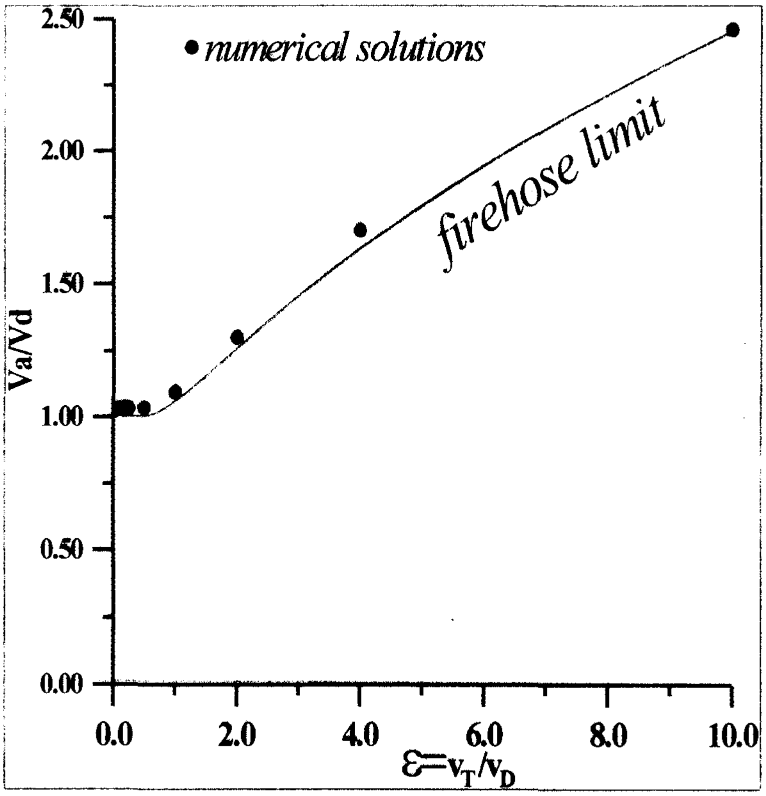

Limit of strong anisotropy

$\varepsilon = v_T/vD << 1$

$$b^2(a) = \frac{2\sqrt{2}}{\pi}\int_0^a (\cos\phi)^{3/2}\, d\phi \int_{a'}^{\infty} da'' \frac{\exp\left(-I_+^{(s)}\right)}{\sqrt{a''-a'}}$$

$$I_+^{(s)} = \frac{2\sqrt{2}}{\pi}\sqrt{\cos\phi}\int_0^{a''}\frac{\sqrt{a''-a'''}}{b(a''')}da'''$$

$$\boxed{a = \int_0^{\zeta} b(\zeta')d\zeta',\ \zeta = \frac{z}{\varepsilon^{4/3}\rho_L}}$$

Scaling of TCS

$L/\rho_L \sim \varepsilon^{4/3}$

(Francfort and Pellat, 1976)

Limit of weak anisotropy

$\varepsilon = v_T/v_D >> 1$

$$\alpha = \varepsilon^{1/3}a,\ \beta(\alpha) = b(a)$$

$$\beta^2(\alpha) = \frac{4}{\pi}\int d^2r \exp\left(-r^2\right)\left\{\left(\int_0^{2y} - \int_{\alpha}^{\alpha+2y}\right)d\alpha'\left(r^2 - I_+^{(w)}\right)\right\}$$

$$I_+^{w} = \frac{2}{\pi}\int_{\alpha''_0}^{\alpha''_1}\frac{\sqrt{y^2+z^2-(y-\alpha'+\alpha'')^2}}{\beta(\alpha)}d\alpha''$$

$$\alpha''_0 = \max\left\{0, \alpha'-y-\sqrt{y^2+z^2}\right\}$$

$$\alpha''_1 = \max\left\{0, \alpha'-y+\sqrt{y^2+z^2}\right\}$$

Scaling

$L/\rho_L \sim 1$

(Ashour-Abdalla, Zelenyi et al.,1994)

$$\xi = \varepsilon^{1/3}\zeta$$

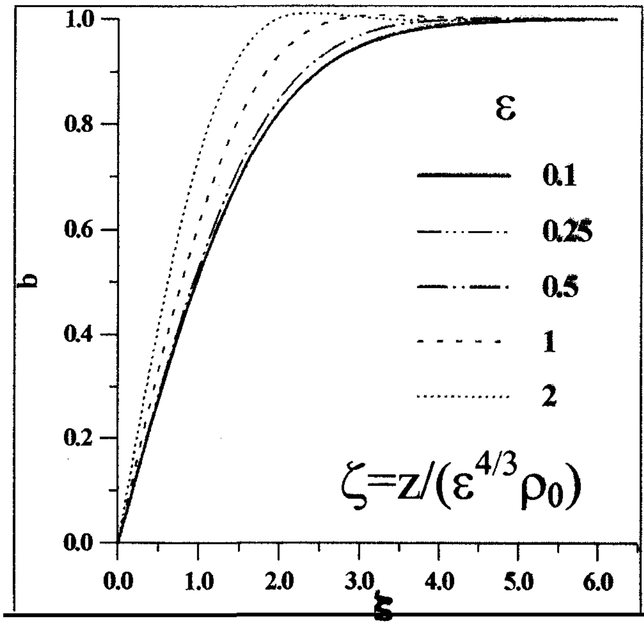

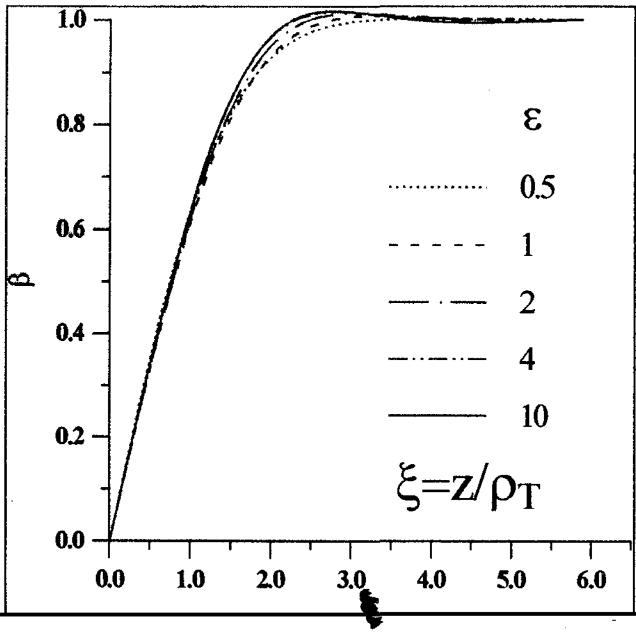

Scaling of TCS

$\varepsilon << 1$: $L \approx \rho_D \varepsilon^{4/3} = \rho_T \varepsilon^{1/3}$
(Francfort and Pellat, 1976)

$\varepsilon \geq 1$: $L \approx \rho_T$ (Ashour-Abdalla, Zelenyi et al., 1994)

$\rho_D = v_D/\omega_0$, $\rho_T = v_T/\omega_0$

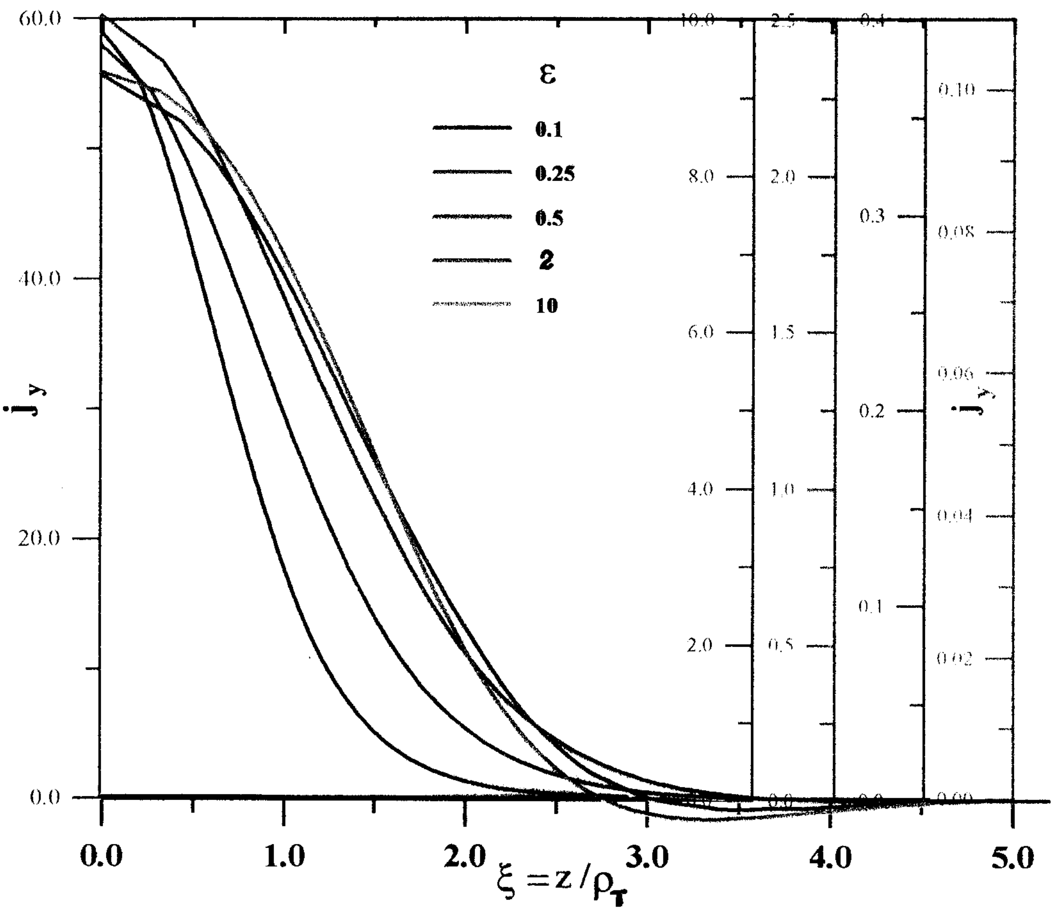

THE SELF-CONSISTENT TCS MAGNETIC FIELDS AND CURRENTS AT DIFFERENT VALUES OF PARAMETER $\varepsilon = V_T/V_D$

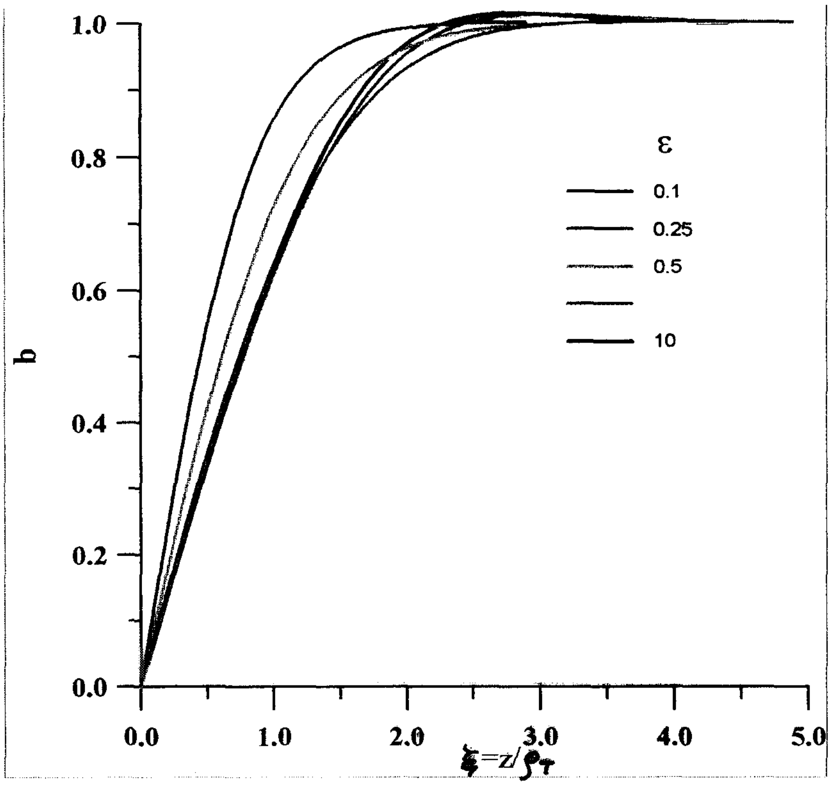

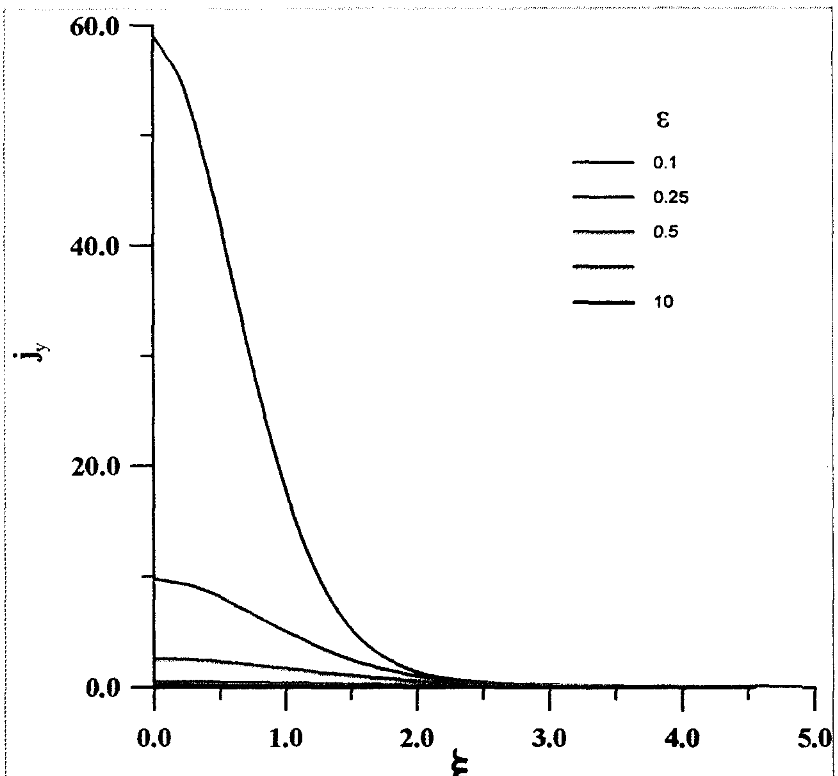

PLASMA DENSITY PROFILES

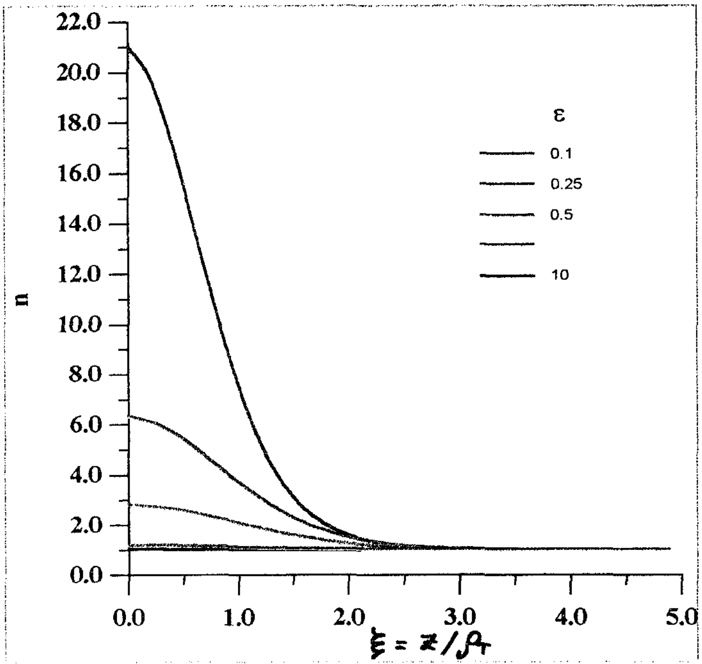

EMBEDDING of TCS into PLASMA SHEET

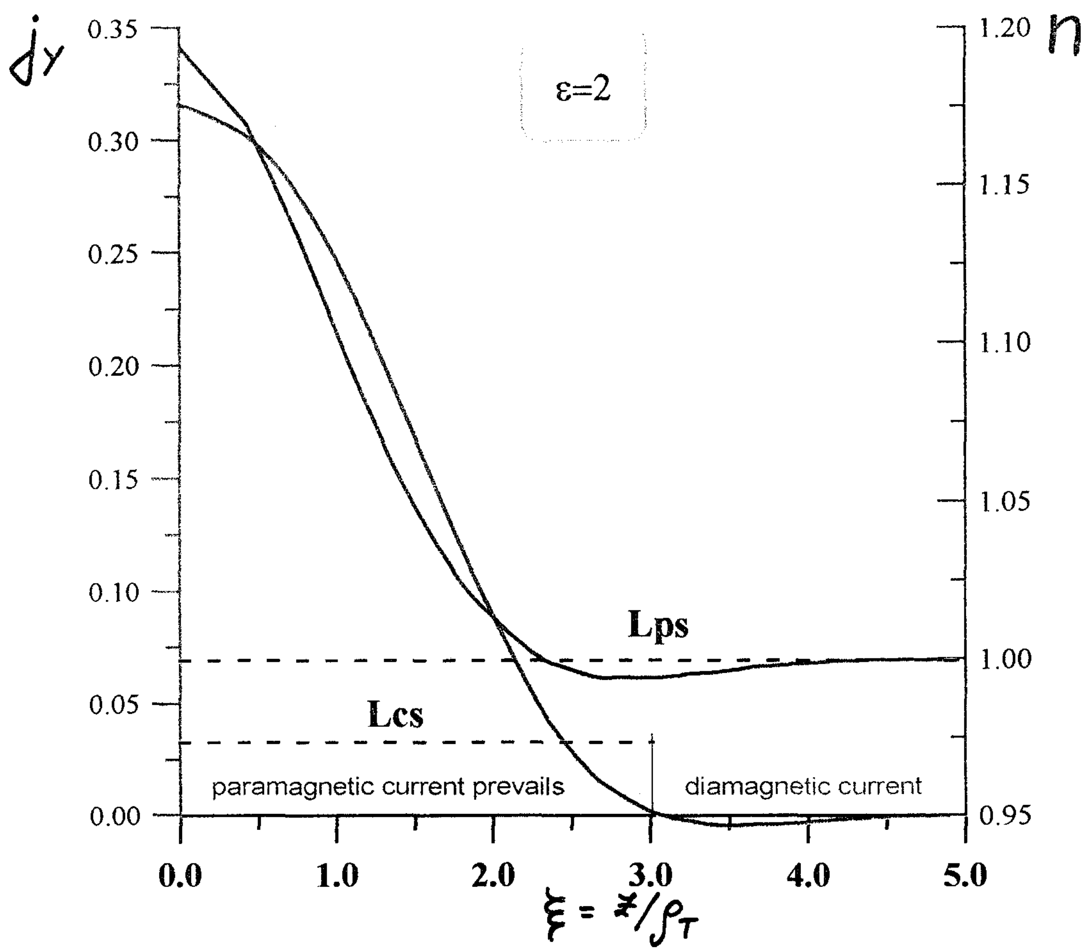

THE UNIFIED PICTURE OF THIN ION CURRENT SHEET SCALING AT DIFFERENT ε.

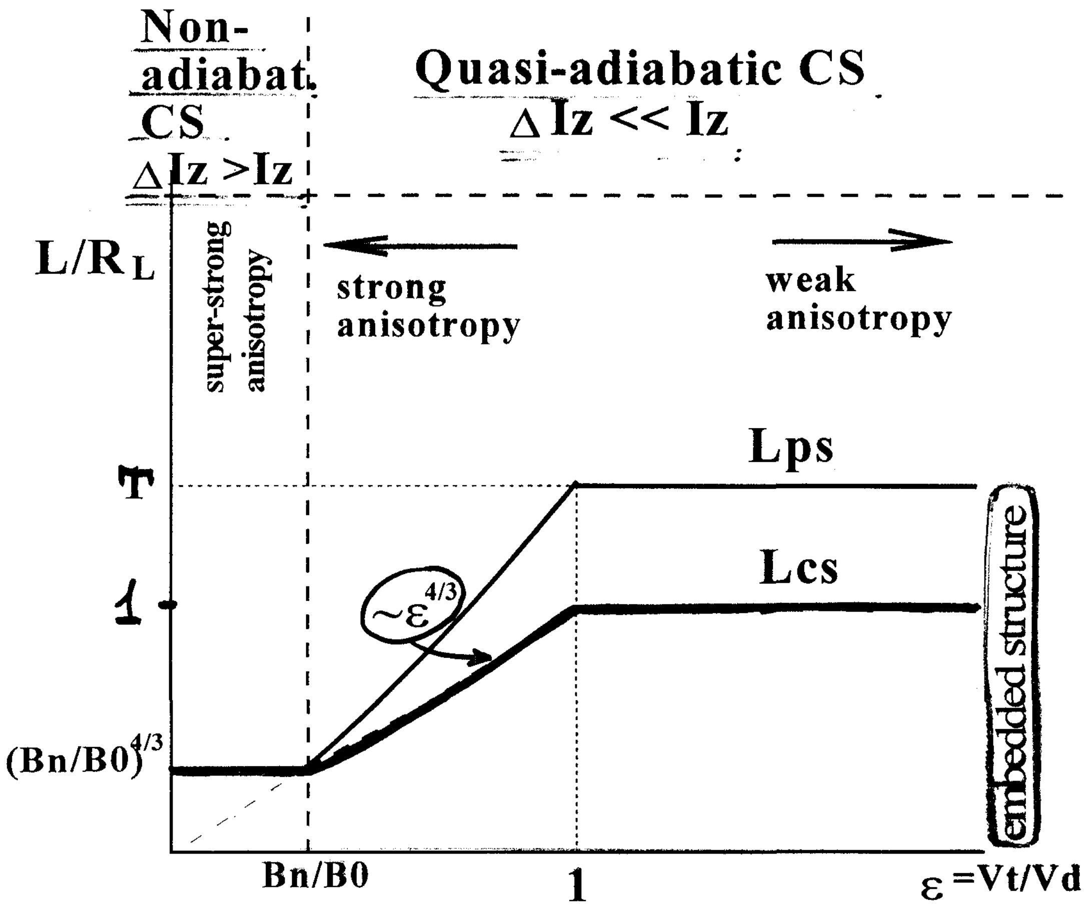

Two kinds of thin ion sheets

1. Quasi-adiabatic CS ($\varepsilon > B_n/B_0$)
2. Non-adiabatic CS ($\varepsilon \leq Bn/B0$).

The analytical model works good in the quasi-adiabatic approximation and doesn't work in non-adiabatic case.

The thickness of PS and CS

The scaling of PS and CS is presented in this picture.

- Weak anisotropy ($\varepsilon>1$). The role of diamagnetic currents is great. The embedded structure is characteristic for the profiles of PS and CS. The thickness of PS is about R_L [Ashour Abdalla, Zelenyi et al., 1994].The thickness of CS is about $0.5R_L$ due to opposite currents competition.

Unified scheme of the selfconsistent current sheet thickness $L\left(\frac{B_n}{B_0}, \frac{V_t}{V_D}\right)$

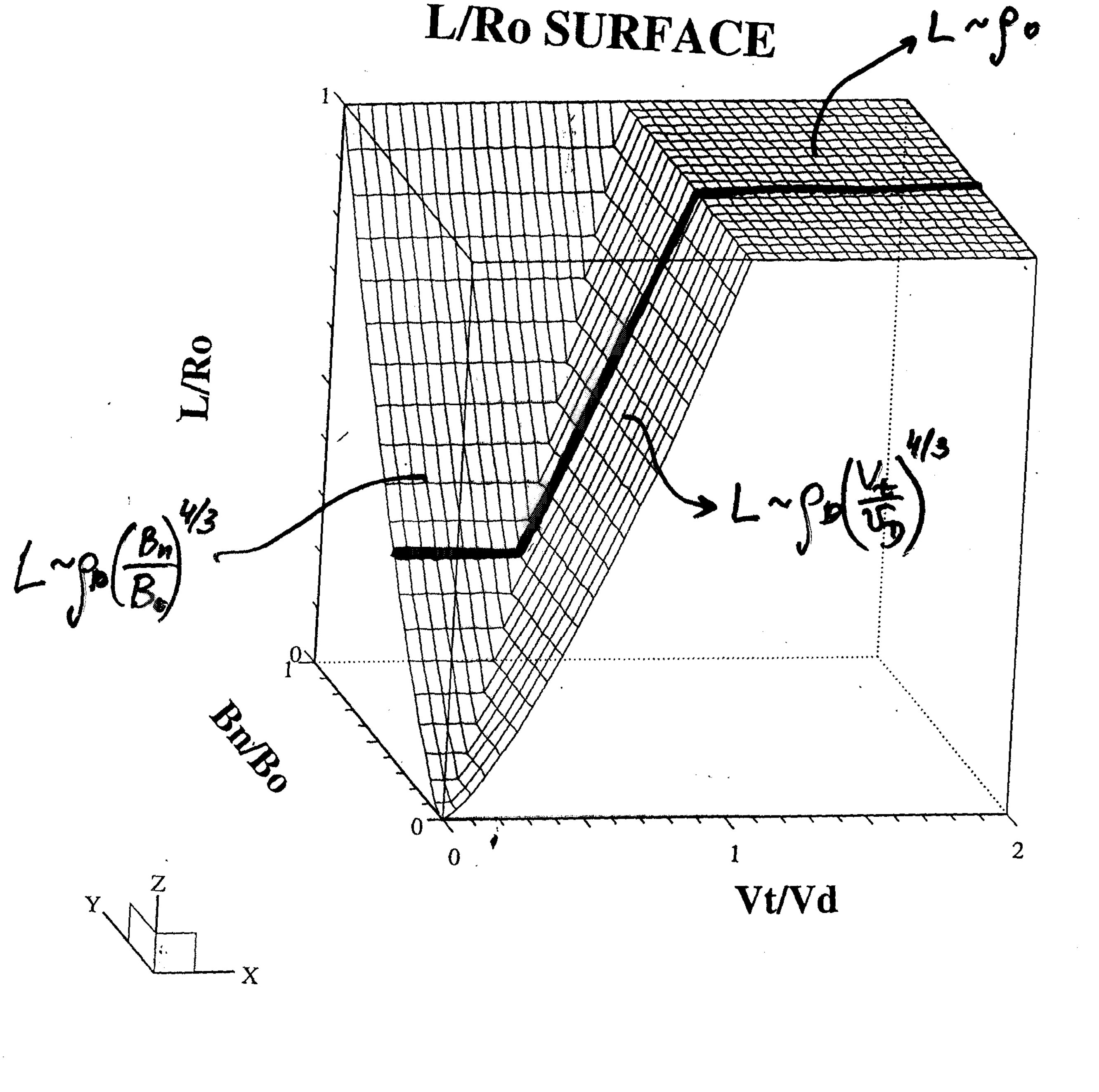

Current Sheet Acceleration

(Shabansky, 1971; Lyons and Speiser, 1982)

$\vec{E}_Y \rightarrow$ *convection* $\rightarrow B_n(x)$ *field*

Nonadiabatic (current sheet) acceleration

Quasi-adiabatic acceleration

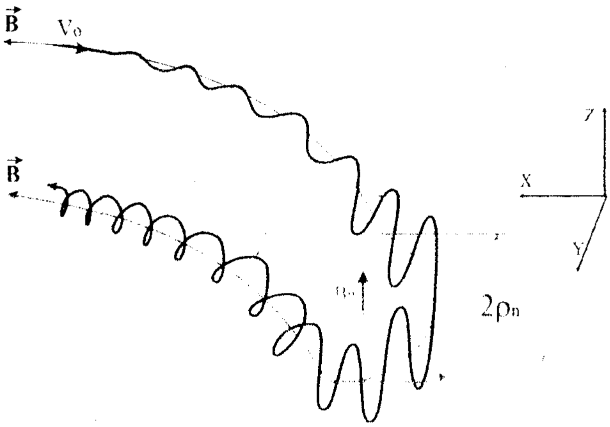

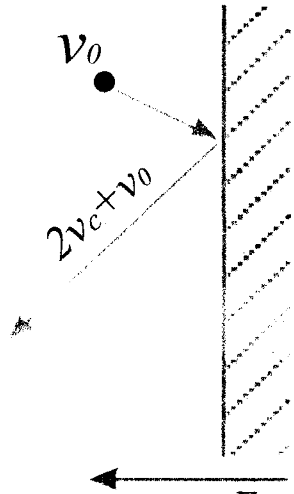

$$v_c = \frac{cE_y}{B_n}$$

deHoffmann-Teller frame

${}_{out} - W_{in} = 2E\Delta y$ $\qquad \boxed{v' = v_0 + v_c}$

$$\Delta y = 2\rho_n$$

$$\rho_n = \frac{v_c}{\Omega_n}, \quad v_c = \frac{cE_y}{B_n}$$

$$(v_{in} = v_0 + v_c \approx v_c)$$

Stationary frame

$\Delta v \cong 2v_c \qquad v_c >> v_0$

$$\Delta W \approx \frac{m_i}{2}(2v_c)^2 = 2m_i v_c^2$$

(Reflection from the Mirror moving with $\mathbf{v_c(x)}$)

$$\Delta W \cong W_{out} \cong 2m_i v_c^2(x)$$

Nonadiabatic energy gain :

$$(x) = 2m_i c^2 \frac{E_y^2}{B_n^2(x)}$$

Problem: W < "thermal" / directed **?**

Role of scattering

33

$$\tilde{E}_y = \frac{c E_y}{v_T B_o}$$

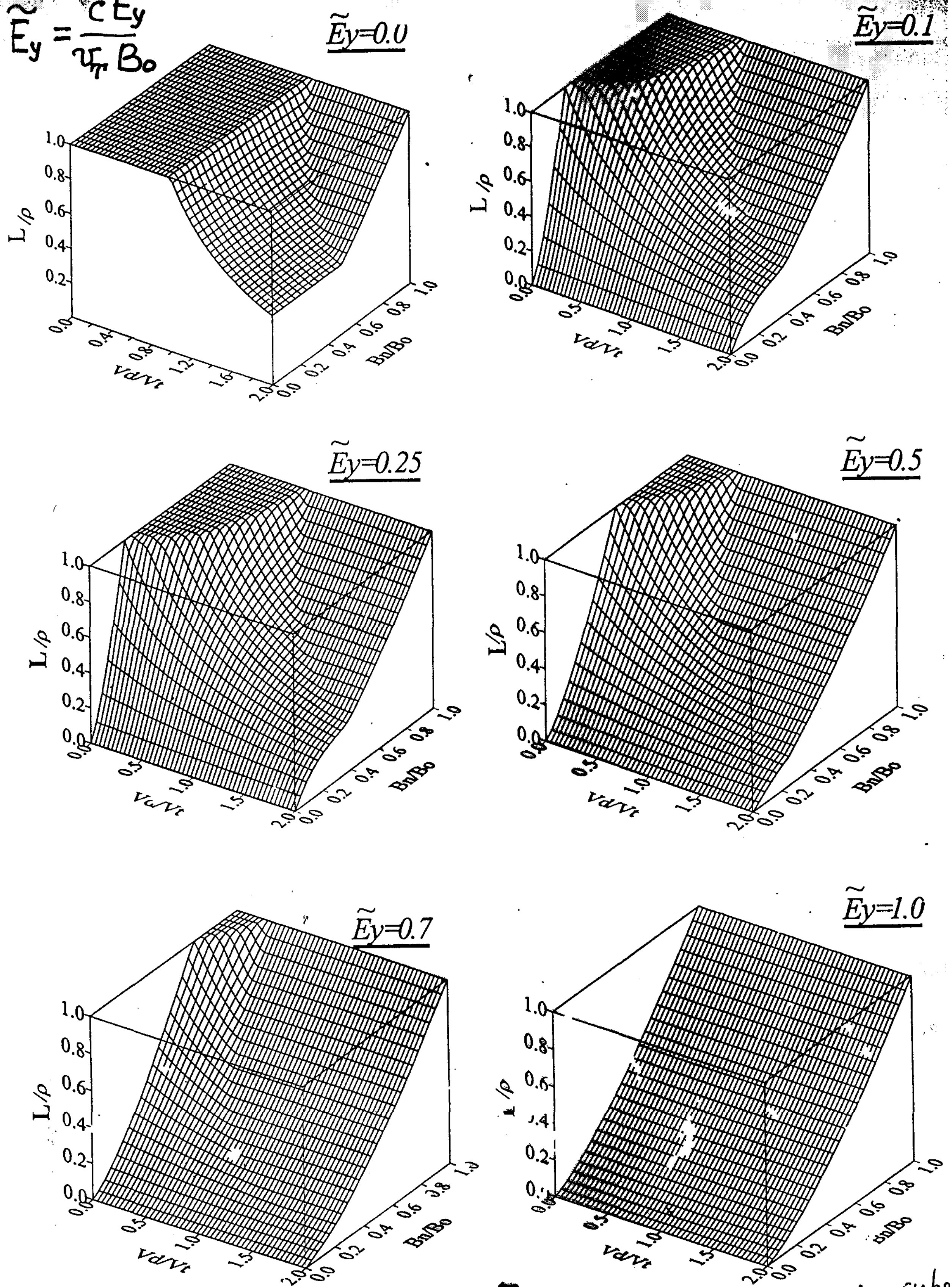

$$V_{\parallel}' = V_{\parallel} + c\frac{E_y}{B_n}$$

$E_y \uparrow$ $L \downarrow$ substorm GROWTH PHASE

Influence of TRAPPED population

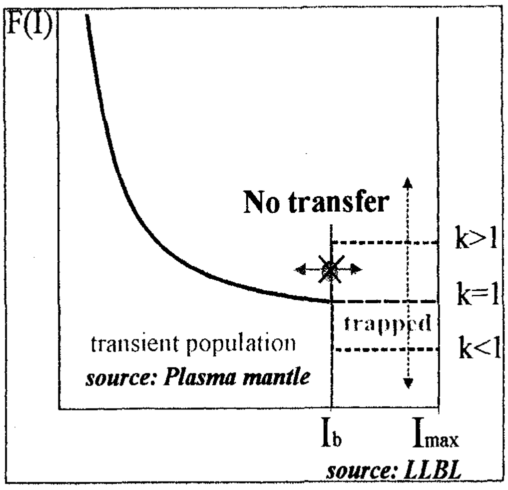

Initial distribution of the transient population:

$$F \sim \exp\left(-\left(V_{II} - V_D\right)^2 + V_\perp^2 / V_T^2\right)$$

$\varepsilon = v_t / v_D$-measure of source anisotropy
v_t is the thermal velocity,
v_D is the drift flow velocity

The initial distribution function of the trapped particles $F \sim k \exp\left(-V_\perp^2 / V_T^2\right)$

Transient (Speiser) orbits

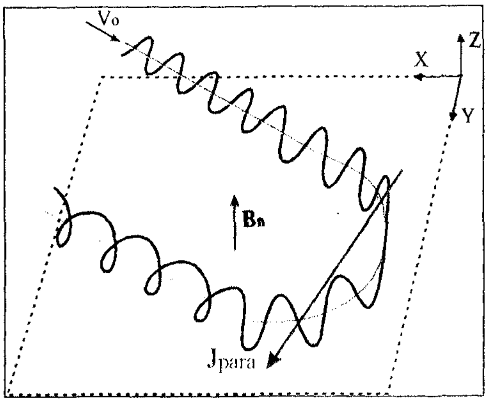

$$I_z \approx const$$

- Create cross-tail current by competition of dia- and para-magnetic effects

$$\langle j_y \rangle \neq 0$$

Trapped orbits

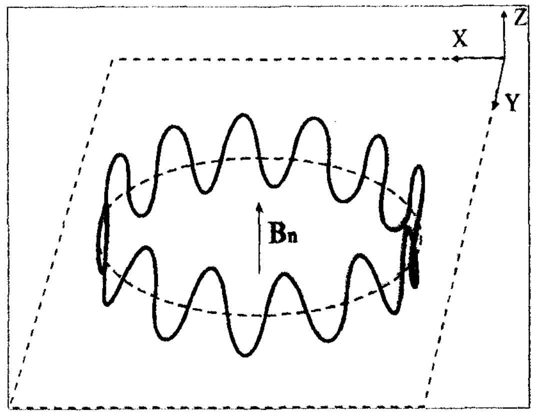

$$I_z \equiv const$$

- Redistribute cross-tail current

$$\langle j_y \rangle = 0$$

INFLUENCE OF THE QUASI-TRAPPED ION POPULATION ON THE TCS EQUILIBRIUM

Trapped population changes:

- the amplitude of the self-consistent **B(z)**
- spatial current structure
  - °decrease of J_{dia} at $z \approx L$
  - °smearing of J_{para} at $z \approx 0$

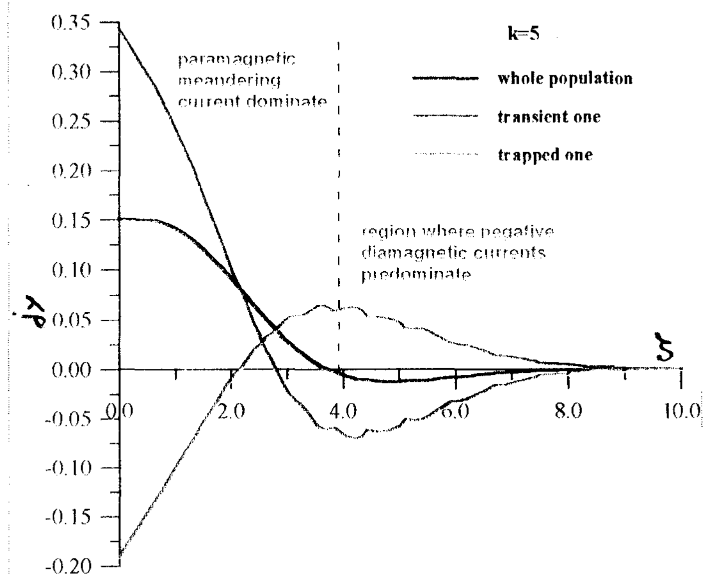

Influence of trapped population (k=0.5; 1; 1.3; 1.4)

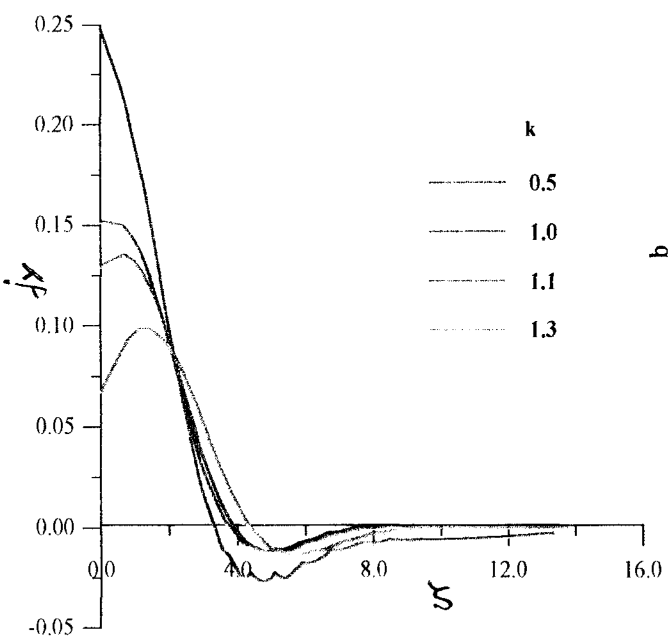

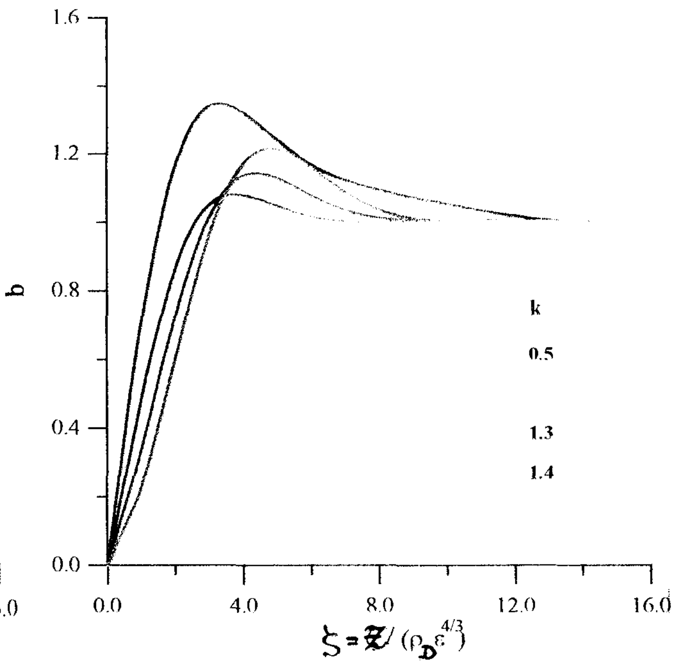

T. Pulkkinen

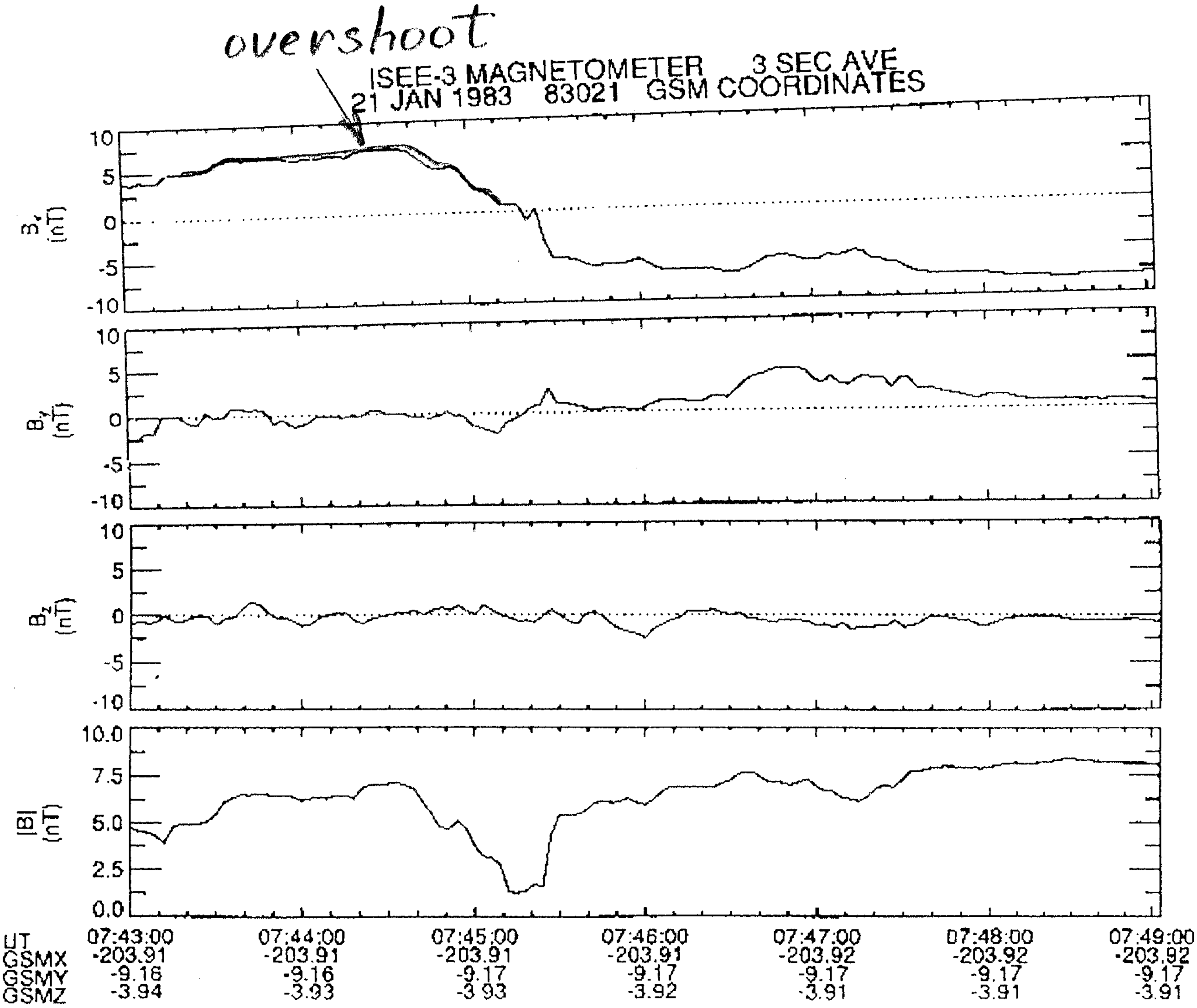
overshoot
ISEE-3 MAGNETOMETER 3 SEC AVE
21 JAN 1983 83021 GSM COORDINATES
Bx (nT)
By (nT)
Bz (nT)
|B| (nT)
10
5
0
-5
-10
10.0
7.5
5.0
2.5
0.0
UT 07:43:00 07:44:00 07:45:00 07:46:00 07:47:00 07:48:00 07:49:00
GSMX -203.91 -203.91 -203.91 -203.91 -203.92 -203.92 -203.92
GSMY -9.16 -9.16 -9.17 -9.17 -9.17 -9.17 -9.17
GSMZ -3.94 -3.93 -3.93 -3.92 -3.91 -3.91 -3.91

Flickering of CS structure

$$\vec{J}_{\perp} = \frac{\vec{B}}{\left|\vec{B}\right|^{2}} \times \left[\vec{\nabla} p + \frac{p_{II} - p_{\perp}}{B^{2}} \left((\vec{B}\nabla)\vec{B} \right) \right]$$

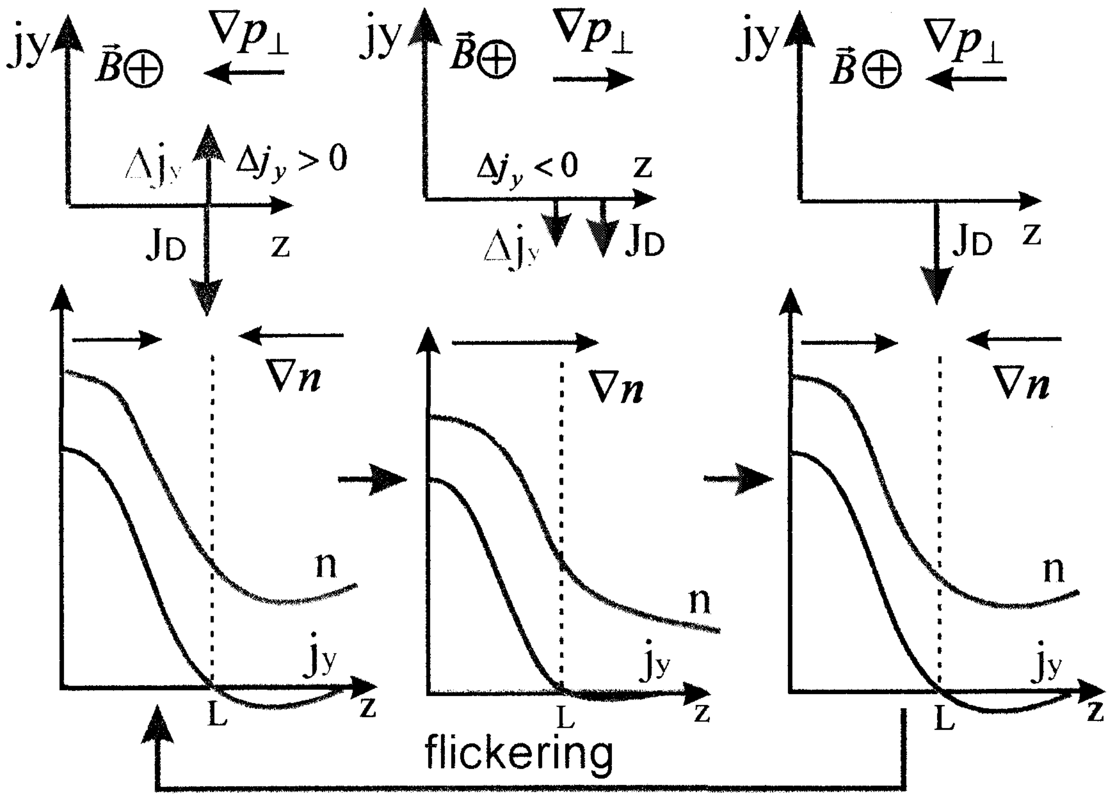

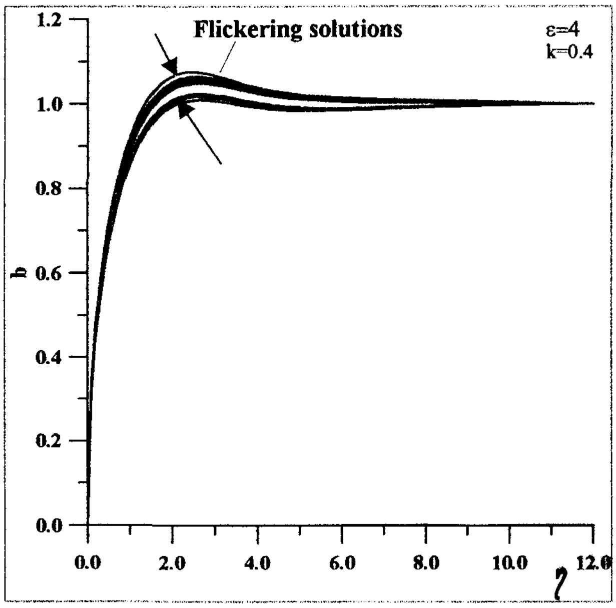

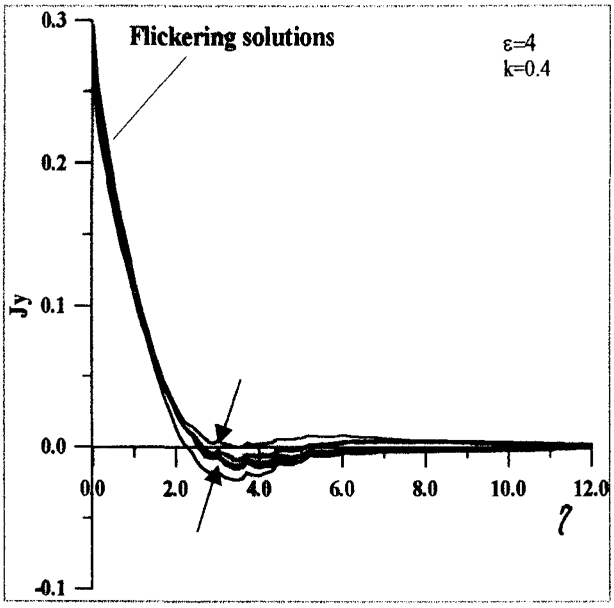

"WINDOW" of SOLUTIONS

$\varepsilon = v_T/v_D$ is the measure of ion streaming;

κ is the measure of trapped population

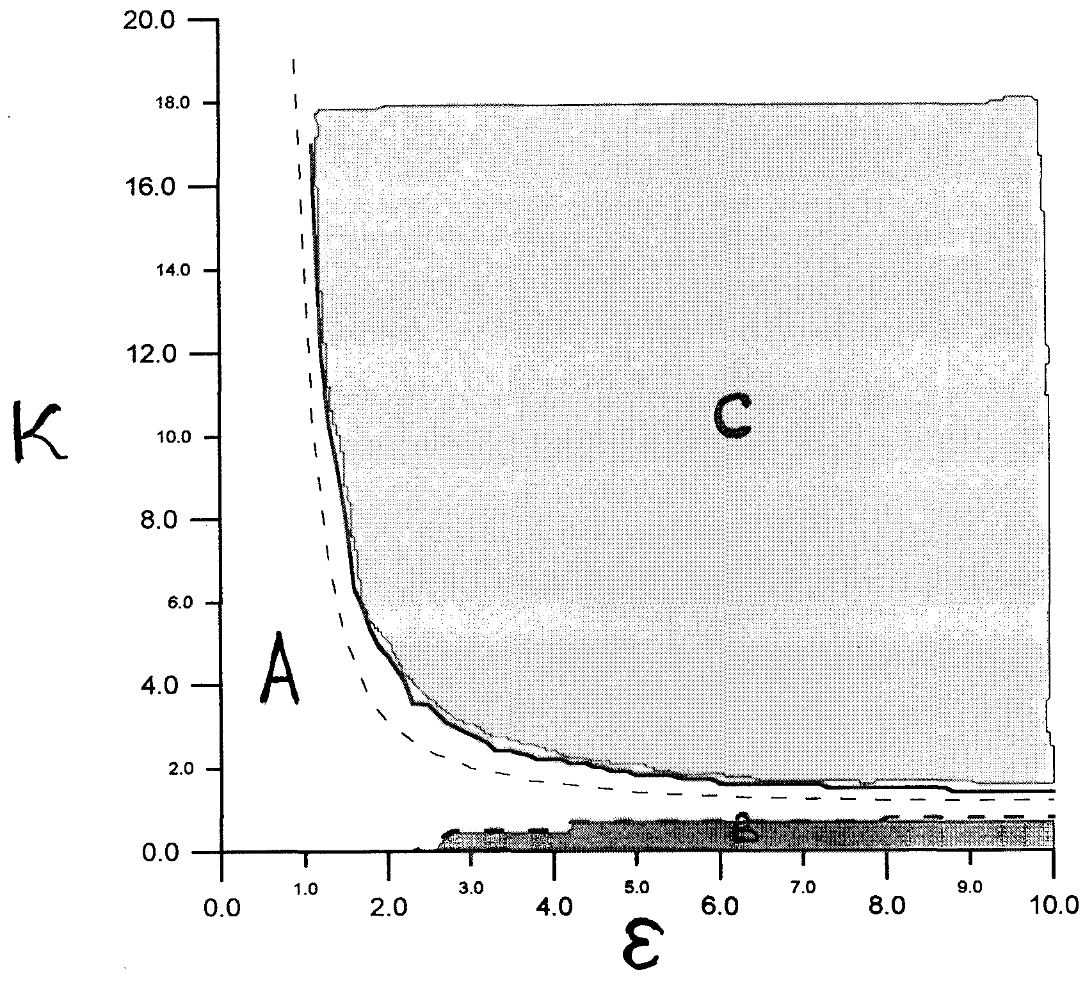

A – Equilibrium solutions

B – Quasi-equilibrium (flickering) solutions

C – No solutions

THE STRUCTURE OF BASIC EQUATIONS (1)-(4)

$F_{(\pm)}$ functions are the contributions of partial currents along the positive and negative Y-axis.

1) The negative current ("diamagnetic"), is due to magnetization current and ion drifts (gradient and centrifugal) in the non-uniform magnetic field, it is created by non-crossing parts of particle orbits and directed along the negative direction (Figure 4).

2)The positive current ("paramagnetic") is carried by meandering part of ion orbits crossing the plane of magnetic field reversal.

In figure below the main constituents of the cross-tail current are illustrated:

A. Non-crossing region, where guiding center approximation could be applied. Schematically are shown: Larmor rotation of particles and their gradient, curvature and magnetization drifts. Net current in this region is negative which illustrates the natural diamagnetism of magnetized plasma.

B. Meandering region of non-guiding center motion. Positive paramagnetic (edge) current is carried by meandering segments of the transit (Speiser) orbits. Particles trapped within CS on specific meandering orbits carry the negative current near the plane $z=0$ and positive current at the edges of their trapping region. At the edges of CS partial compensation of paramagnetic current by diamagnetic drift currents could occur

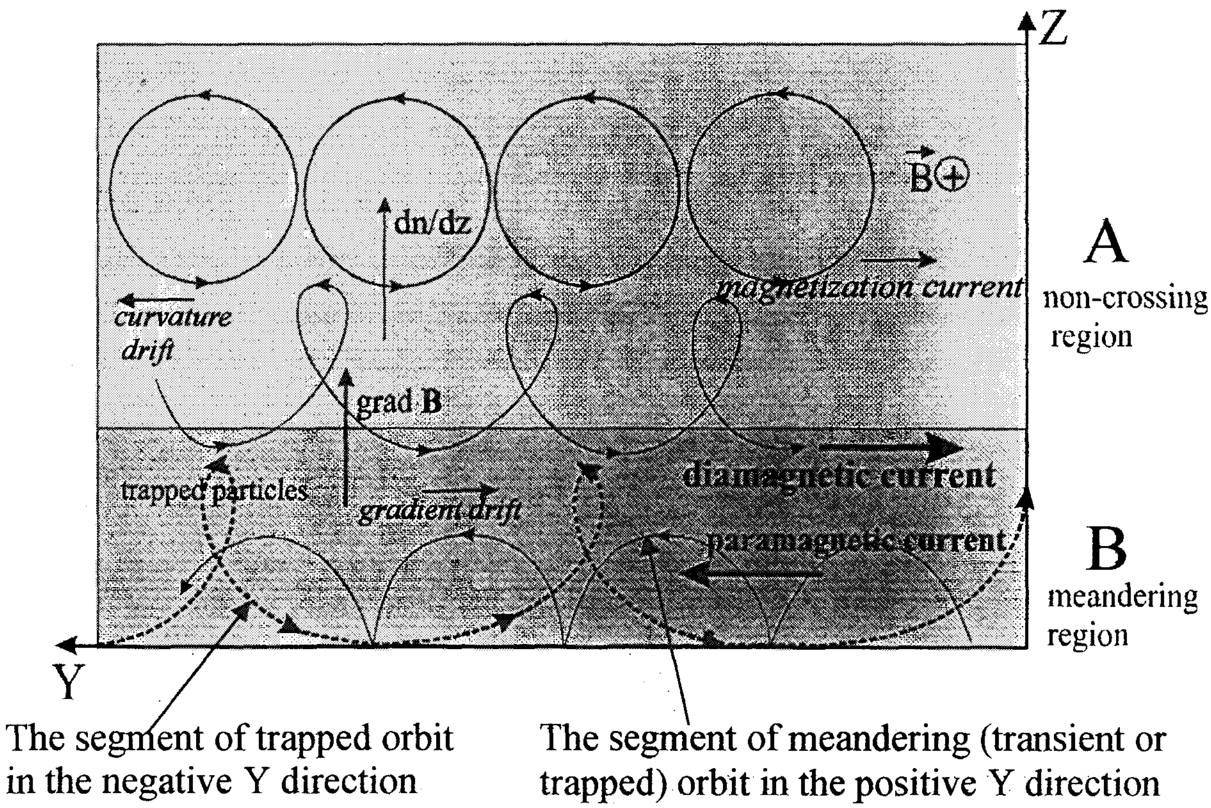

Harris equilibrium.

$$f_{0j} = \frac{n_0}{ch^2(z/L)} \exp\left(\frac{m_j[(\mathrm{v}_x - V_0)^2 + (\mathrm{v}_y - u_j)^2 + \mathrm{v}_z^2]}{2T_j} \right)$$

$$\frac{u_e}{T_e} + \frac{u_i}{T_i} = 0, \qquad L = \frac{c}{\omega_{pi}} \frac{\mathrm{v}_{Ti}}{u_i} \sqrt{\frac{T_i}{T_e + T_i}}$$

Bulk velocity (V_0) along **B** does not influence current sheet structure.

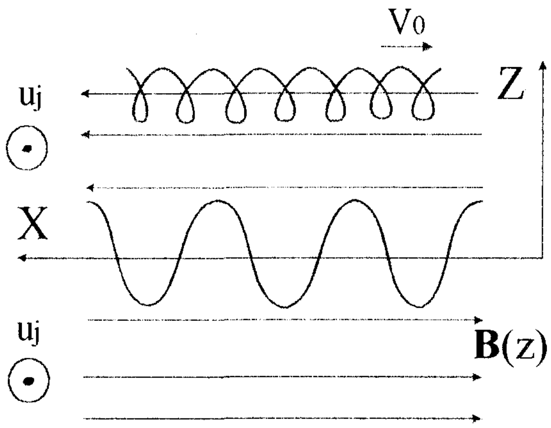

uj - diamagnetic drift velocity

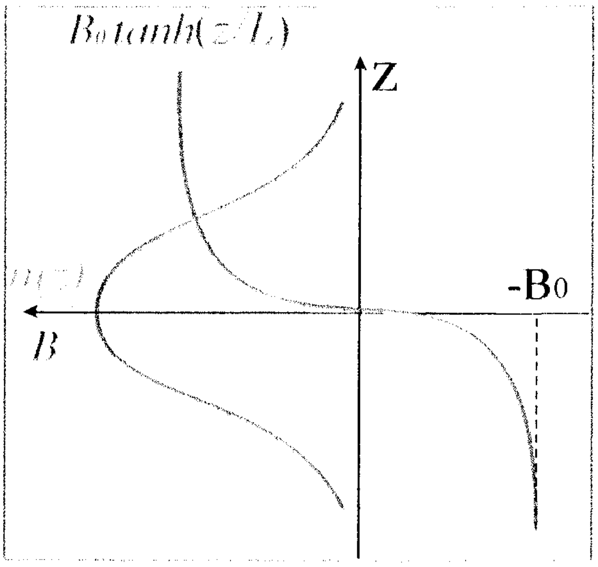

PROFILES of current and density ***<u>COINCIDE</u>***

$$B_x = B_0 \tanh\left(\frac{z}{L}\right) \quad : \quad \frac{B_0^2}{8\pi} = n_0\left(T_{e\perp} + T_{i\perp}\right)$$

$$n(z) = \frac{n_0}{ch^2\left(z/L\right)}$$

$$J_y(z) = \sum_j e_j n_j u_j = \frac{c}{B^2}\left|\vec{B} \times \nabla p_{\perp j}\right| = \frac{J_0}{ch^2\left(z/L\right)}$$

- diamagnetic current

DIAMAGNETIC versus PARAMAGNETIC current sheets

$$J_{\perp j} = q_j nc \frac{[\vec{E} \times \vec{h}]}{B} + \frac{c}{B}[\vec{h} \times \nabla p_{\perp j}] + \frac{c}{B}(p_{II} - p_{\perp})[\vec{h} \times (\vec{h}\nabla)\vec{h}]$$

• DIAMAGNETIC CURRENT

• Guiding center particles: ANISOTROPIC CURRENT

Non-adiabatic particles: PARAMAGNETIC CURRENT

$\vec{h} = \vec{B}/|B|$

<u>*Harris sheet:*</u> $L_{HS} \sim \frac{v_{Ti}}{u_i} \sim \left(\frac{\partial p}{\partial z}\right)^{-1}$

made from Diamagnetic currents (supported by LOCAL pressure gradients)

Filamentation

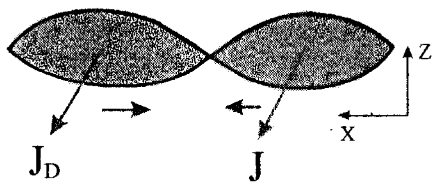

Kinking

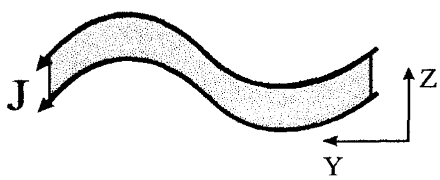

<u>*FORCED CURRENT SHEETS*</u>

supported by paramagnetic currents
(due to pressure anisotropy)
could be more STABLE vs. TEARING/KINK MODES

Harris CS → Anisotropic CS

- Even infinitely small value of $\mathbf{B_n}$ drastically changes the structure of equilibrium.
- Meandering region becomes dynamically accessible from the lobes.
- Current sheet structure becomes dependent on $v_{||} \leftrightarrow v_{\perp}$ anisotropy.
- Existence of $B_n \to 0$ transforms the properties of equilibrium solution (even if B_n does not explicitly enter the final equations)

CONCLUSIONS

1. We consider the class of self-consistent equilibriums of thin current sheets ($L<\rho_{0i}$) with magnetic tension balanced by centrifugal force $(\vec{B}\nabla)\vec{B}$.

2. CS structure is determined by the competition of DIA- and PARAmagnetic effects

$\Rightarrow$ The overshoot structure of the magnetic field profile is characteristic for weak anisotropic TCS.

3. Flux of TRAPPED particles is a free parameter which essentially control the structure of CS, although $\langle j_y \rangle_{TR} \equiv 0$

4. TRAPPED population suppresses

* Paramagnetic current within CS

* Diamagnetic current of transient particles at the edges of CS

4a. As a result steady solutions exist in a window of parameters (ε,k)

ε - *measure of anisotropy,* k *- measure of the trapped population*

5. Trapped population occupies the well-defined domains in the phase space which could be identified by the *in situ* measurements of ion distribution function $f_i(v)$ in the vicinity of the field reversal.

6. There are many indications on the existence of the dynamics (flickering) quasi-equilibriums.

REFERENCES for LECTURE 2

A. Results of Lecture 2 are published in following papers:

1. Zelenyi L.M., M.I.Sitnov, H.V.Malova, S.Sharma. Thin and superthin ion current sheets. Quasi-adiabatic and nonadiabatic models. J. Nonlinear Processes in Geophysics, 7, 3/4, 127-139, 2000

2. Sitnov M.I., L.M.Zelenyi, H.V.Malova, S.Sharma. Thin current sheet embedded within a thicker plasma sheet: Self-consistent kinetic theory. J.Geophys.Res., **105**, A-6, 13.029-13.044, 2000

3. Malova H.V., M.I.Sitnov, L.M.Zelenyi, S.Sharma. Self-consistent model 1D current sheet: the role of drift, magnetization and diamagnetic currents. AGU, Geophys. Monograph 118, Magnetospheric Current Systems, 313-322, 2000.

4. Zelenyi, L.M., A.Galeev, and C.F. Kennel, Ion Precipitation From the Inner Plasma Sheet Due to Stochastic Diffusion, J. Geophys. Res., 95, 3871, 1990.

5. Ashour-Abdalla, M., L. M. Zelenyi, V. Peroomian, and R. L. Richard, On the structure of the magnetotail current sheet, Geophys. Res. Lett., 20, 2019, 1993.

6. Zelenyi, L. M., B. V. Savenkov. Violating of Quasiadiabaticity During the Particle Motion in Magnetic Field Configurations with Strongly Curved Field Lines. Plasma. Phys. Rep. (Transl.from Russian), 19, 712, 1993.

7. Savenkov, B.V., L.M. Zelenyi. Application of Separatrix Crossing Theory to Nondiffusion Model of Current Sheet Resonance. Geophys. Res. Lett., 23, 3255 , 1996.

8. Vainshtein D.L., L.M. Zelenyi, A.I. Neishtadt, B.V. Savenkov. Jumps in an adiabatic invariant with small initial values. Plasma Phys. Rep., **25**, 4, 290-303, 1999, Transl. from Fizika Plazmy, 25, 4, 333-337, 1999.

B. Additional important publications:

1. Harris, E. G., On a Plasma Sheath Separating Regions of Oppositely Directed Magnetic Fields, Nuovo Chimento, 23, 115, 1962.

2. Eastwood, J. W. Consistency of fields and particle motion in the 'Speiser' model of the current sheet. Planet. Space Sci., 20, 1555-1568, 1972.

3. Speiser T. W. Conductivity without collisions or noise. Planet. Space Sci., 18, 613, 1970.

4. Sonnerup B.U.O. Adiabatic particle orbits in a magnetic null sheet. J. Geophys. Res., 76, 8211, 1971.

5. Syrovatsky, S.I. On the Appearance of Current Sheet in Plasma with Frozen-in Strong Magnetic Field. Sov. Phys. JETP, 60, 1727, 1971.

6. Burkhart G.R., Drake J. F., Dusenbery P. B., Speiser T. W. A particle model for magnetotail neutral sheet equilibria. J. Geophys. Res., **97**, 13799-13815, 1992.

7. Rich F.J., Vasyliunas V.M., Wolf R.A. On the balance of stresses in the plasma sheet. J. Geophys. Res., **77**, 4670-4676, 1972.

8. Pritchett P. L., Coroniti F. V. Formation and stability of the self-consistent one-dimensional tail current sheet. J. Geophys. Res., 97, 16773-16787, 1992.

9. Lyons, L. R., T. W. Speiser. Evidence for current sheet acceleration in the geomagnetic tail. J. Geophys. Res., 87, 2276, 1982.

10. Frankfort P, R.Pellat. Merging in collisionless plasma. Geophys. Res. Lett. 3, 433, 1976.

11. Pulkkinen T. I., Baker D. N., Mitchell D. G., McPherron R. L., Huang C. Y., Frank L. A., Thin current sheets in the magnetotail during substorms: CDAW 6 revisited, J. Geophys. Res., 99, 5793, 1994.

12. Holland, D.L., J. Chen. Self-consistent current sheet structures in the quiet-time magnetotail. Geophys. Res. Lett., 20, 1775--1778, 1993.

13. Kaufmann, Richard L., Ball, Bryan M., Paterson, W. R., Frank, L. A. Plasma sheet thickness and electric currents. J. Geophys. Res., **106**, A4, 6179-6194, 2001

14. Shabansky V.P. Space Sci. Res., 3, 12, 1971.

C. TEXTBOOKS

1. Bateman G., MHD instability, The MIT Press Cambridge, Massachusetts, and London, England, 1979.

2. Dendy R. Plasma Physics: an Introductory Course, Published by Press Syndicate of the Univ. Cambridge, Cambridge University Press , N.-Y., USA, 1993.

3. Krall N.A., A.W. Trivelpiece. Principles of plasma physics, McGraw-Hill Book Company, N.-Y., 1973

4. Nicholson, D.R., Introduction to plasma theory, Ed. By J.Wiley&Sons, Inc., N.-Y., USA, 1983

5. Sturrock P.A., Plasma Physics, Published by the Press Syndicate of the University of Cambridge, Cambridge University Press , N.-Y., USA, 1994.